HEAT WAVE ASSOCIATED WITH SURFACE OZONE POLLUTION IN DELHI

A DISSERTATION SUBMITTED IN PARTIAL FULFILMENT OF THE

REQUIREMENTS FOR THE AWARD OF DEGREE

FOR

MASTER OF TECHNOLOGY

IN

ENVIRONMENTAL ENGINEERING

Submitted by

MOHAMMAD ARSH HANIF CHAUDHRY

2K20/ENE/06

Under the supervision of

DR. GEETA SINGH

DEPARTMENT OF ENVIRONMENTAL ENGINEERING

DELHI TECHNOLOGICAL UNIVERSITY

(Formerly Delhi College of Engineering)

Bawana Road, Delhi-110042

MAY 2022

DELHI TECHNOLOGICAL UNIVERSITY

(Formerly Delhi College of Engineering)

Bawana Road, Delhi-110042

CANDIDATE'S DECLARATION

I, Mohammad Arsh Hanif Chaudhry, Roll No. 2K20/ENE/06 student of M. Tech (Environmental Engineering), hereby declare that the project Dissertation titled "Heat wave associated with surface ozone pollution in Delhi" which is submitted by me to the Department of Environmental Engineering, Delhi Technological University, Delhi in partial fulfillment of the requirement for the award of the degree of Master of Technology, is original and not copied from any source without proper citation. This work has not previously formed the basis for the award of any Degree, Diploma Associateship, Fellowship or other similar title or recognition.

Place: Delhi MOHAMMAD ARSH HANIF CHAUDHRY

Date:

DELHI TECHNOLOGICAL UNIVERSITY

(Formerly Delhi College of Engineering)

Bawana Road, Delhi-110042

CERTIFICATE

I hereby certify that the Project Dissertation titled "Heat wave associated with surface ozone pollution in Delhi" which is submitted by **Mohammad Arsh Hanif Chaudhry, Roll No. 2K20/ENE/06**, Department of Environmental Engineering, Delhi Technological University, Delhi in partial fulfillment of the requirement for the award of the degree of Master of Technology, is a record of the project work carried out by the student under my supervision. To the best of my knowledge this work has not been submitted in part or full for any Degree or Diploma to this University or elsewhere.

Place: Delhi **DR. GEETA SINGH**

Date: **SUPERVISOR**

ACKNOWLEDGEMENT

I want to express my deepest gratitude to my supervisor Dr. Geeta Singh, Assistant Professor, Department of Environmental Engineering, Delhi Technological University, New Delhi, for her guidance, help, useful suggestions and supervision without which this report could not havebeen possible in showing a proper direction while carrying out project. I also must acknowledge the unconditional freedom to think, plan, execute and express, that I was given in every step ofmy project work, while keeping faith and confidence on my capabilities.

MOHAMMAD ARSH HANIF CHAUDHRY

2K20/ENE/06

ABSTRACT

Heat waves are expected to grow more extreme across most worldwide land regions as greenhouse gas levels continue to rise and average temperatures rise in both trials (greater maximum temperatures during heat waves). It was hypothesized that heat waves are associated with surface ozone levels. To test this hypothesis correlation and regression analysis were used across Delhi using the air quality data from 4 monitoring stations run by CPCB. The ozone concentrations have been studied for monthly and seasonal patterns. Dependence of surface ozone concentration on $PM_{2.5}$, PM_{10}, NO, NO_X, CO, SO_2, Relative Humidity, Ambient Temperature, and Wind Speed has been studied. The role of ozone precursors and reduction in $PM_{2.5}$ and NO_X have been illustrated. Significant association was found among temperature and ozone further it was observed that Ozone concentrations fluctuate throughout the day, for different study period. Additionally, the role of NO_X, VOCs and solar radiations in ozone formation have been discussed.

Keywords: ArcGIS, Heat Wave, Heat Index, Ground Level Ozone

TABLE OF CONTENTS

LIST OF TABLES

LIST OF FIGURES

ABBREVIATIONS

O_3	Ozone
VOCs	Volatile Organic Carbon
SO_2	Sulfur Dioxide
NO_2	Nitrogen Dioxide
NO	Nitric Oxide
μgm^{-3}	Microgram per meter cube
CPCB	Central Pollution Control Board
$PM_{2.5}$	Particulate Matter less than 2.5-micron size
PM_{10}	Particulate Matter less than 10-micron size
GHGs	Green House Gases
RH	Relative Humidity
WS	Wind Speed
AT	Ambient Temperature
σ	Standard Deviation

Chapter 1

INTRODUCTION

1.1. Heat Wave

Heatwave as a disaster-causing hazard is little more than the physical phenomena of extreme heat, and is defined as a complex of hydro-climatic dangers, as well as social, occupational, and public health concerns. A Heat Wave is a period of exceptionally high temperatures, above the typical maximum temperature, that happens in the North-Western areas of India during the summer season.

Heatwaves usually occur between March and June, with some occurrences lasting into July. Extreme temperatures and the ensuing climatic conditions have a negative impact on those who live in these areas because they produce physiological stress, which can lead to mortality. As a result, no general definition of a heatwave exists. A protracted period of high heat is the most common definition.

As seen in the diagram, the Indian Meteorological Department (IMD) specifies the following criteria for Heat Waves - Heat Waves should not be included until a station's maximum temperature reaches at least 40°C for Plains and at least 30°C for Hilly areas. Heat Wave Departure from Typical is 4^{o}C to 5^{o}C when a station's normal maximum temperature is greater than 40^{o}C, and Severe Heat Wave Departure from Normal is 6^{o}C or more. Heatwaves should be declared when the actual highest temperature is 45°C or above, regardless of the typical maximum temperature.

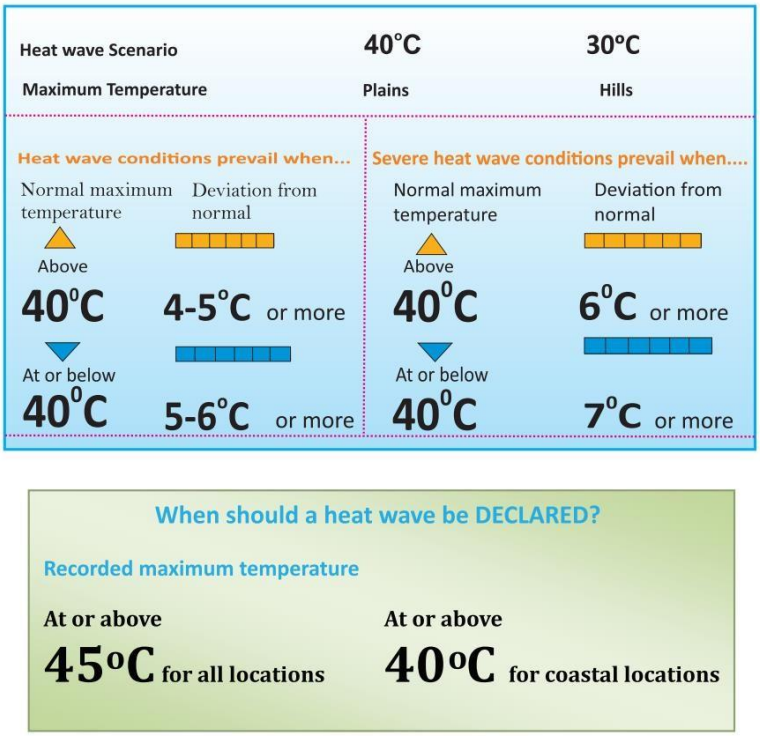

Figure 1.1 Identifying a heat wave in India

More than 2,300 people died in India's heat wave in 2015, making it the world's fifth deadliest in terms of death toll. Andhra Pradesh, Telangana, Punjab, Odisha, and Bihar were the states with the most deaths. Figure 2 shows how global temperatures continued to rise in 2016.

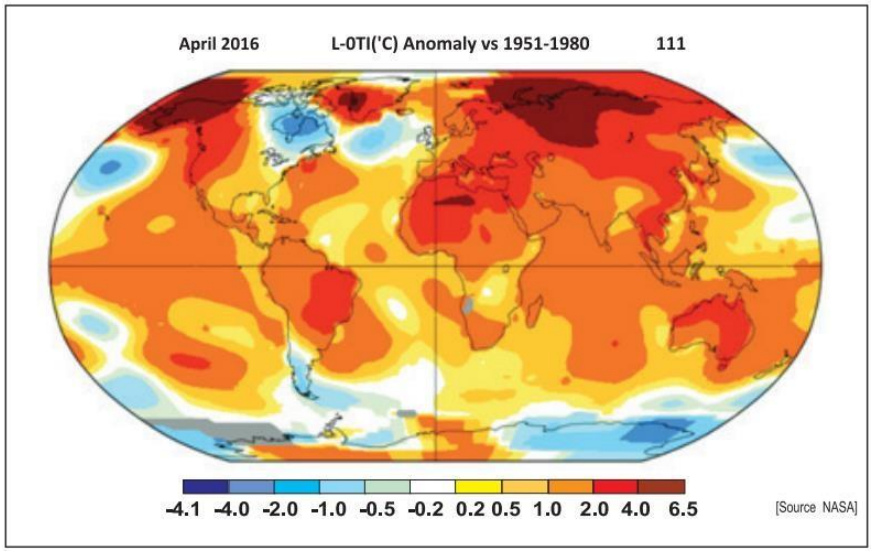

Figure 1.2: Global Heat wave conditions in April 2016

For example, the month of April 2016 witnessed the highest average worldwide temperature ever recorded. As seen in Figure 3, India had one of the most severe heat waves in April 2016, contributing to a large number of heat-related deaths.

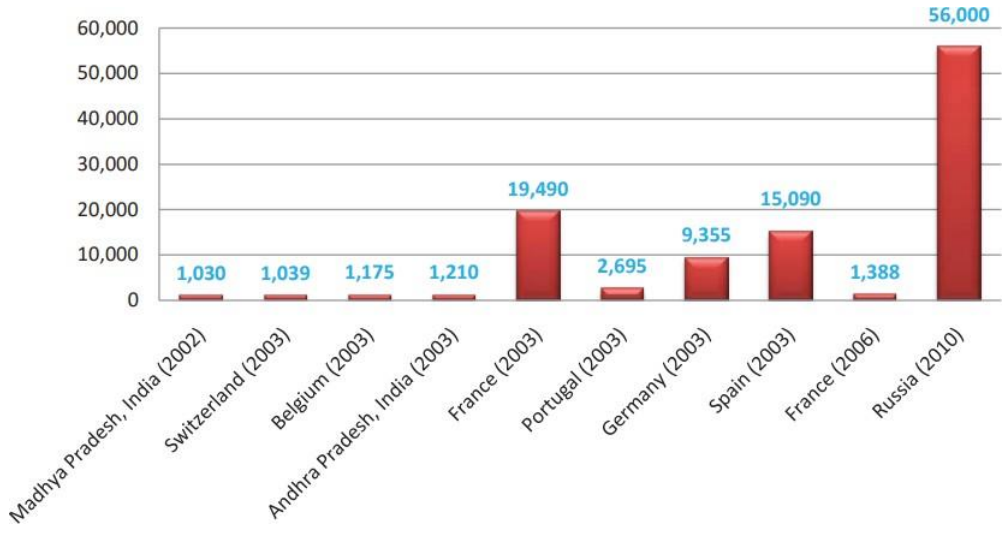

Figure 1.3: Ten highest Mortality Heat events across globe (2001-2010)

Heat discomfort is determined by a number of elements, including: meteorological - air temperature, relative humidity, wind direction, and direct sunlight; cultural - clothes, occupation, and lodging; and physiological - health, fitness, age, and acclimatization level (ability to adapt). As a result, vulnerability assessments must be conducted in order to collect reliable data on morbidity, comprehend practices and cultural behavior in order to build suitable strategies, Mapping community-level capacities and resources for intervention in design, gaining a better understanding of how various government initiatives are perceived and used, identifying the most vulnerable people and developing action plans for them. measures should be taken to mitigate and prepare for vulnerable populations, redesigning disadvantaged people's livelihoods or working environments, summertime population, heat-friendly city planning techniques and policies should be adopted.

1.1.1. Heat Wave in India

Heat has major health consequences in India. Since 1992, there have been approximately 22,000 heat-related deaths in India, according to estimates. As seen in Table 1, the country experienced the seventh worst heat wave in history in 2015 (EM-DAT, 2015). In addition to the above-mentioned vulnerable populations, the poor may be disproportionately affected due to deficits in health care, housing, and basic necessities. Furthermore, the urban heat island effect makes Indian cities susceptible. For example, urban development increases built-up areas, which generate heat emissions, as well as impermeable surfaces and longer travel distances, which result in more vehicle trips and air pollution. Temperatures might rise by 1-2°C as a result of the significant anthropogenic component, reinforcing positive feedback loops through increased air conditioning. During the months of March to June, a heat wave sweeps across the plains of NW India, East, Central and North Peninsular India. States and Union territories like Delhi, Haryana, Punjab, UttarPradesh, West Bengal, Madhya Pradesh, Jharkhand, Rajasthan, Odisha, Gujarat and Bihar. Tamil Nadu and Kerala are also included. However, high temperatures of greater above 45°C were recorded primarily in Rajasthan and Gujarat.

Table 1.1: Year-wise Death Cases of Heat Waves during 2005-2015

Sl. No	DISTRICT	2010	2011	2012	2013	2014	2015
1	MEDAK	NA	NA	7	24	2	35
2	MAHABUBNAGAR	NA	NA	2	27	0	42
3	NALGONDA	0	1	0	209	22	139
4	KARIMNAGAR	NA	NA	22	91	0	120
5	RANGAREDDY	NA	NA	0	11	0	36
6	ADILABAD	NA	NA	44	43	7	26
7	NIZAMABAD	5	0	2	36	0	18
8	KHAMMAM	NA	NA	42	35	0	95
9	HYDERABAD	0	0	0	0	0	10
10	WARANGAL	6	NA	25	40	0	20
TOTAL		11	1	144	516	31	541

1.1.2. Causes of Increasing Heat Wave Incidences

The intensity of the heat waves is also connected to less pre-monsoon rain showers in many locations, since there has been far less moisture than usual in that area, leaving significant swathes of India barren and dry. The heat waves have been exacerbated by the abrupt cessation of pre-monsoon rain showers, which is an unusual occurrence in India. The El Nino influence, which generally raises temperatures in Asia, teamed with this weather trend to produce record high temperatures. The impacts of the high humidity on the inhabitants were amplified by the high temperatures.

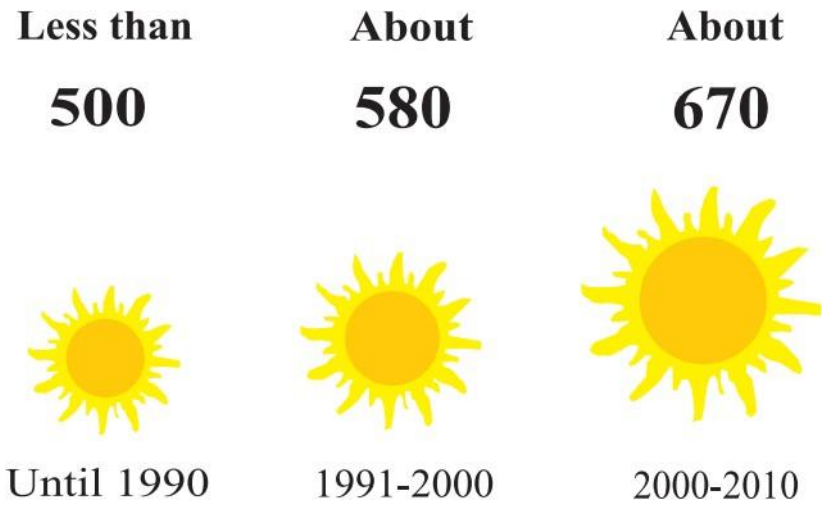

Figure 1.4: Heat waves in India/year (Source: Indian Meteorological Department)

El Nino is a Pacific Ocean climate cycle that influences numerous weather systems throughout the world. It's a phenomenon that occurs as warmer water from the western tropical Pacific Ocean moves eastward down the equator, eventually reaching the western coast of South America by mid-December. The year after this December phenomena is known as a 'El Nino year,' since it shows the impacts of the Pacific Ocean warming that was observed in 2015. During an El Nino year, India usually experiences drought, with areas relying only on rainfall and poor irrigation when the South West monsoon dries up.

According to reports, high pressure zones in the Arabian Sea and Indian Ocean in the south Indian peninsula worked as a trigger for the North East monsoon in 2015, resulting in more rainfall in Tamil Nadu and other parts of the South peninsula than in the previous three years. The majority of India is reliant on the South West monsoon.

El Nino and Indian Monsoon precipitation are often negatively connected. During the Southwest Monsoon, trade winds from South America generally sweep westward towards Asia, but as the Pacific Ocean warms, these winds lessen.

As a result, moisture and heat content are restricted, resulting in less rainfall and unequal distribution throughout the Indian subcontinent. Since 1871, six of the most notable droughts in India have been produced by El Nino, including the most recent ones in 2002 and 2009. Nonetheless, it's worth noting that not all El Nino years result in drought in India.

1.1.3. Heat Wave's Health Effects

Heat syncope, heat cramps, heat exhaustion, and heat stroke are the four primary medical conditions caused by excessive exposure to heat waves. The following are the indications and symptoms: Heat rash, often known as sunburn, is characterized by reddish skin that burns and causes pain, Giddiness, vertigo headache, and abrupt onset drowsiness/unconsciousness are all symptoms of heat syncope, Heat Cramps: Edema (swelling) and Syncope (fainting) are usually associated with a temperature of less than 39°C (102°F), Fatigue, weakness, disorientation, headache, nausea, vomiting, muscular cramps, and sweating are all symptoms of heat exhaustion, Heat Stoke: Body temperatures of 40 degrees Celsius (104 degrees Fahrenheit) or higher, as well as delirium, convulsions, or coma. These may prove to be life-threatening.

1.1.4. Heat Index (HI) classification and health effects

The increased frequency and intensity of extreme weather events expected for the future as a result of climate change is causing considerable worry in the scientific and public health sectors. The

Heat Index, commonly known as the apparent temperature, is the temperature that the human body perceives when relative humidity and air temperature are combined. Evaporation is a cooling process with significant implications for human comfort. When the body becomes too heated, it begins to sweat or perspire to cool down. The body cannot regulate its temperature if sweat does not evaporate. The rate of sweat from the body reduces when the ambient moisture content (i.e., relative humidity) is high, thus the human body feels warmer under humid situations.

Table 1.2: Heat Index (HI) classification and health effects

Heat Index	Category	Health Effects
27 – 32°C	Warm	Caution- Fatigue possible with prolonged exposure and/or physical activity. Continuing activity could result in heat cramps
32 – 41 °C	Hot	Extreme caution- Heat cramps and heat exhaustion possible with prolonged exposure and/or physical activity
41 – 54 °C	Very Hot	Danger- Heat cramps or heat exhaustion likely and heatstroke possible with prolonged exposure and/or physical activity
> 54 °C	Extremely Hot	Extreme danger- Heatstroke highly likely with continued exposure

1.2. Ozone

The color less gas ozone is made up of three oxygen atoms. Ozone is created through chemical interactions between natural and man-made emissions of nitrogen oxides (NOx) and volatile organic compounds (VOCs) in the presence of sunlight, rather than being discharged directly into the air. When these gaseous components combine with sunlight, they generate ozone, which looks like a thin soup in the ambient, or outside, air. There are two forms of ozone: stratospheric ozone and ground-level ozone.

1.2.1 Stratospheric ozone

When strong sunlight causes oxygen molecules (O_2) to break apart and re-form as ozone molecules, stratospheric ozone, commonly known as the "ozone layer," occurs high in the atmosphere, 6-30 miles above the earth's surface (O_3). The ozone layer is made up of these ozone molecules, which are referred to as "good ozone." Ozone protects and shelters people, plants, crops, property, and microbes from the destructive effects of the sun's UV radiation at concentrations as high as 12,000 ppb (the EPA considers anything above 70 ppb to be dangerous for human health and welfare).

1.2.2 Ground-Level Ozone

Ground-level ozone is produced just above the earth's surface (up to 2 miles above ground) and has an influence on human, animal, and plant respiration. Despite the fact that ground-level ozone is less concentrated than stratospheric ozone, its negative effects on human health and welfare make it "bad ozone." Ozone at ground level is an irritant that can harm human health and wellbeing. The weather has a significant impact on the development of ground-level ozone. Ground-level ozone concentrations are normally greatest on hot/humid days with low humidity and little or no wind. As early as March and as late as October, ozone concentrations in Central Texas reach levels that are deemed "unhealthy for sensitive groups."

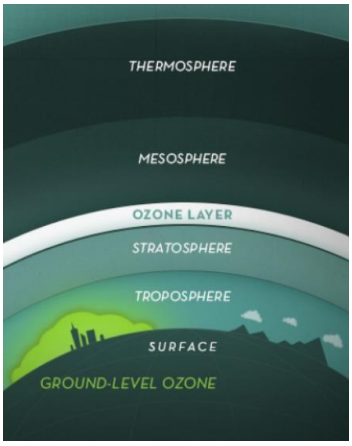

Figure 1.5: Atmospheric layer

1.2.2.1. What are the consequences of ground-level ozone on human health?

The ground level ozone or Bad Ozone may have severe health impacts to exposed human population. The major effects are listed below:

- Make breathing deeply and forcefully more difficult.
- When taking a deep inhale, cause shortness of breath and suffering.
- Causing coughing and a scratchy or painful throat
- Inflammation and injury to the lungs
- Lung illnesses include asthma, emphysema, and chronic bronchitis get worse.
- Asthma episodes will become more frequent.
- Increase the risk of infection in the lungs
- Even after the symptoms have gone away, continue to harm the lungs.
- Chronic obstructive pulmonary disease

These consequences may result in more school absences, doctor appointments, and emergency department visits, as well as hospital admissions. Ground-level ozone exposure has also been linked to an increased risk of early mortality from heart or lung illness, according to research.

Ozone sensitivity varies from person to person. Children, the elderly, and persons with lung diseases such as asthma, emphysema, and chronic bronchitis are among the most vulnerable groups. Even healthy persons who engage in outdoor activities might be affected by ozone.

1.2.2.2. What other impacts does ground-level ozone have on the environment?

Ground-level ozone makes it difficult for people to breathe, but it also makes it difficult for plants to breathe. The EPA's 2015 Ozone National Ambient Air Quality Standards are designed to preserve human health as well as the public welfare, which includes vegetation. According to the EPA, ground-level ozone reduction can have the following effects on vegetation:

- Keep forest communities safe.

- Increase wood and agricultural production, such as soybeans and winter wheat.

1.2.2.3. The policy background for ground-level ozone

During the second part of the twentieth century, the impacts of O_3 on human health and the environment led to the establishment of regulations and control mechanisms in a number of nations. The scope of this paper does not allow for a full examination of the efficacy of control measures; nonetheless, the primary implications of the policies within the nations to which they apply and on the worldwide distribution of O_3 are discussed.

Ground-level O_3 pollution was first recognized in California in the 1950s, and it was thought to be a local and regional problem. Control efforts aimed to limit O_3 precursor emissions, with an emphasis on peak concentrations, which were thought to be the most harmful to human health and ecosystems. Throughout the 1970s, harmful O_3 concentrations in other regions of North America, Europe, and Japan were more widely recognized, prompting national and regional measures to restrict precursor emissions.

1.3 Why studying surface ozone pollution is necessary?

Ozone is a difficult contaminant to measure and control due to its complex chemistry. Ambient ozone is not directly emitted from any source at ground level. It is created when nitrogen oxides (NOx) and volatile organic compounds (VOCs) are emitted from automobiles, power plants, industries, and other combustion sources and undergo cyclic reactions in the presence of sunlight to form ground level ozone. Natural sources of VOCs, such as plants, can also emit them. Ozone is a greenhouse gas that traps heat. Ozone not only forms in cities, but it also travels vast distances to become a regional pollution, necessitating both local and regional response. Mitigation necessitates strict gas management from all combustion sources. As a result, while designing particulate matter mitigation, it is also required to calibrate the action strategy for reducing ozone precursors. This highly reactive gas can be hazardous to one's health. Those with respiratory

disorders, such as asthma or chronic obstructive pulmonary disease (COPD), as well as children with premature lungs and elderly adults, are more vulnerable. This can irritate and damage airways, expose lungs to infection, aggravate asthma, emphysema, and chronic bronchitis, and increase the frequency of asthma attacks, resulting in more hospitalizations. This necessitates exposure control whenever ozone build-up occurs. This is why, unlike other pollutants, the threshold for ground level ozone has been defined for hourly and eight-hourly duration.

Chapter 2

LITERATURE REVIEW

As per (Hendriks et al., 2016), (Anshika et al., 2021) and (Lu et al., 2020a), surface ozone is harmful to human health and decreases crop production. According to WHO, 2013, short-term exposure to high ambient O_3 and long-term exposure to low levels both raise the risk of respiratory and cardiovascular disorders (Fleming et al., 2018). The principal source of surface ozone is the oxidation of volatile organic compounds (VOCs) in the presence of nitrogen oxides (NOx). Rapid economic development in India has considerably boosted emissions of these O_3 precursors, resulting in considerable increases in O_3, particularly during the pre-monsoon period (Ghude et al., 2008). During the pre-monsoon season in Delhi, hourly maximum O_3 levels reach as high as 140 pp bv (Ghude et al., 2008), equivalent to the most polluted districts in China (150 ppbv; (Wanget al., 2017) and higher than the most contaminated locations in the United States (110 pp bv; (Luet al., 2020b).

(Sharma et al., 2019) studied the variations of surface ozone in Delhi's atmosphere. According to the research, an anomaly variance, there has been a considerable positive increase in day time and nighttime surface ozone concentrations since 1998, with deviations from the mean reaching 29.91 ppb for 2007 (daytime) and 10 ppb for 2010. (night-time). From 1990 to 2012, the annual average distribution of data revealed a progressive increase in ozone levels over the research area. The mean night-time ozone concentration increased over time, exceeding 18 ppb in 2010, while the mean concentration ranged between 3 and 4 ppb during the study period. According to the observed trends, there is a direct link between daytime concentrations and higher nighttime surface ozone levels. The Mann Kendall test confirmed the growing trend, revealing a statistically significant trend at the 95 percent significance level with a Sen's slope of +0.158. Using the ARIMA model, the author projected the trend of both surface and night-time ozone concentration

levels over Delhi until the year 2025, taking into account the implications of increasing levels of surface ozone in the atmosphere. Between 2013 and 2025, the model's results revealed an upward trend in both surface and night-time ozone concentration levels. Numerous variables could be contributed to the city's high and increasing levels of night-time ozone, according to the trend analysis and literature assessment conducted in the study. As a result, the author focused on recognising the need of identifying numerous sources and reducing the city's increasing surface ozone concentration. Furthermore, the research was a significant contribution that would pave the way for discussions on the significance of residual ozone deposition, as well as the importance of night-time chemistry and meteorology, in understanding the impact of surface ozone on agriculture, climate, and human health.

A study was conducted by (PAI et al., 2013) on trends of heat waves in India over a span of 50 years. Various statistical characteristics of heat waves (HWs) and severe heat waves (SHWs) like long term climatology, interannual variability, and long-term trends were evaluated using HW data from 103 stations across India during the hot weather season (March to July) during the previous 50 years (1961-2010). The relationship between HWs/SHWs and the ENSO phenomenon, which was linked to weather patterns all over the world, was also investigated. Many parts of the country (the N, NW, central, and NE peninsulas) have had HW days of about 8 days per season on average. The SHW mostly affected the country's north, northwest, and central regions. Over the last four decades, there had been a considerable increase in the number of HW/SHW days compared to the prior four decades. During the recent decade 2001-2010, which was also the country's and the world's warmest decade, there was a considerable increase in HW/SHW days over the country compared to the previous four decades. During the analyzed period, significant long-term increases in HW days were also seen over India. Around 25 sites in north, northwest, and central India showed a substantial increase in HW days, while 5 stations, mostly in northwest India, showed a large increase in SHW days. Few locations, however, have

demonstrated a considerable decrease in HWs and SHWs (2 stations from north India and 3 stations from the east coast) (2 stations from east coast).

With the dimming impact of aerosols and the elimination of hydroperoxy radicals are reduced, allowing O_3 synthesis, $PM_{2.5}$ pollution mitigation may result in an increase in surface ozone (Li et al., 2019) (Qu et al., 2021). Furthermore, reducing NOx and $PM_{2.5}$ emissions together may boost O_3 production in cities where O_3 production is limited by VOCs (Ran et al., 2009; Xing et al., 2017, 2018). This has lately been documented in a number of Asian megacities, including Shanghai (Silver et al., 2018), Beijing (Liu et al., 2017); (Chen et al., 2018) and Hong Kong (Liaoet al., 2021). Increased O_3 could be a side effect of $PM_{2.5}$ emission limits in Delhi and coastal towns in India, which are known to be VOC-limited (Hakkim et al., 2019).

Excess mortality is caused by elevated surface ozone concentrations, which impair human health through asthma and other respiratory problems, especially during excessive heat (Levy & Patz, 2015). Ozone is also a potent oxidant that impairs the physiology of most plants (Lombardozzi et al., 2015), affecting agricultural production (Chuwah et al., 2015a), as well as global carbon and water cycles (Lombardozzi et al., 2015). Surface ozone is formed when volatile organic compounds and carbon monoxide (CO) are oxidized in the presence of nitrogen oxides (NOx), with enhanced reactivity at higher temperatures, resulting in a significant relationship between surface temperature and surface ozone concentrations,(Camalier et al., 2007) and (Bloomer et al.,2009). As a result, high temperatures are frequently linked to heightened surface ozone and its detrimental consequences (Fiore et al., 2015).

Previous studies have revealed projected reductions in summer surface ozone concentrations in scenarios that predict future reductions in anthropogenic ozone precursor emissions.(Shen et al., 2016) and (Phalitnonkiat et al., 2018) found geographical differences in the likelihood of future heat waves and high surface ozone concentrations in the United States. In the present-day climate

over various parts of the United States, heat and severe surface ozone episodes have been related (Huang et al., 2017), (Lu et al., 2019), (Sun et al., 2017).

However, no research has been done on how future heat waves (e.g., (Meehl & Tebaldi, 2004), (Perkins-Kirkpatrick & Gibson, 2017) would affect surface temperatures. Furthermore, no studies have compared the reactions in places where ozone precursor emissions are expected to fall significantly (e.g., most of North America and Europe under RCP6.0) with areas where precursor emissions are expected to grow or vary little (e.g., most of Asia in this scenario).

The development of ozone precursors controls just a portion of the link between surface ozone concentration and heat waves. When greater temperatures do not necessarily result in increased surface ozone concentrations, ozone suppression can occur. Reduced isoprene emissions due to biophysical restrictions at high temperatures and ozone production saturation from the decomposition of peroxyacetyl nitrate (PAN), a NO_x reservoir, are two possible explanations (Steiner et al., 2010) , (Sun et al., 2017).

The Representative Concentration Pathway (RCP) scenarios used in global climate models to anticipate future climate change forecast the future development of anthropogenic ozone precursor emissions (e.g., NOx, CH_4, CO, VOCs) (Lamarque, 2005), (Dufresne et al., 2013). Globally averaged ozone precursor emissions drop in all RCP scenarios, while there is significant regional variation based on estimates about air pollution legislation in various nations. Regulationsrequiring more widespread use of catalytic converters in automobiles, NOx control policies, and policies supporting the replacement of petrol-based cars with electric vehicles are examples of the sorts of measures used to reduce ozone precursor emissions (at least in OECD nations).

According to (Pfister et al., 2014) reducing ozone precursor emissions by 20% under RCP8.5 (a scenario with greater greenhouse gas emissions than RCP6.0 but equivalent ozone precursor emissions) leads in a 20% reduction in summer mean daily maximum 8 hourly average ozone concentration (MDA8) across the US.

When ozone precursors (and consequently surface ozone concentrations) do not decline as stipulated in the RCP scenarios, an IAM has been used to demonstrate future increases in surface ozone concentrations (Chuwah et al., 2015b). The relationship between summer heat waves and elevated surface ozone have been studied by many researchers on comprehensive and interactive tropospheric and stratospheric chemistry - in which ozone concentration depends on various ozone precursors as well as changes in transport and dynamics.

As previously stated, all RCP scenarios anticipate worldwide reductions in numerous ozone precursors as a result of expected policy improvements, although this leads to increases in certain locations and decreases in others (van Vuuren et al., 2011), (Eyring et al., 2013). The influence on the association between heat waves and ozone if ozone precursors do not alter in the future as a result of these actions is the second topic we investigate. To answer this question, we run a different set of simulations with anthropogenic ozone precursors set to their 2005 levels to see how ozone precursor variations impact the link between heat waves and surface ozone concentrations.

Chapter 3

METHODOLOGY

3.1 STUDY AREA

The site selected for this study is the National Capital Territory of Delhi. Delhi (28.7041° N, 77.1025° E) has a vast population of 3.2 crore with a population density of 10,000 people per Km^2 (Census-2011). Delhi has an altitude of 216 m above mean sea level with area spreading up to 1485 Km^2. Summers in Delhi are extremely hot, while winters are extremely chilly. The temperature ranges from 45 degrees Celsius in the summer to 3 degrees Celsius in the winter. The mornings are characterized by mist and fog, and the afternoons are frequently sunny. Winters are bitterly cold due to a cold surge from the Himalayan region. Since decades, the city of New Delhi has been a hotbed of human activity. The summer and autumn seasons have the highest ozone concentrations, while the monsoon and winter seasons have the lowest. Throughout the year, diurnal trends in ozone concentration reveal daytime in situ photochemical production. Days with high ozone levels were linked to weather conditions such as bright and warm weather, stagnant wind patterns, and low relative humidity. The hourly averaged surface ozone levels in Delhi, on a large number of days have been found to exceed the World Health Organization (WHO) ambient air quality standards (hourly average of 80 ppb) for ozone. Delhi's atmosphere sees a substantial makeup of tropospheric ozone and many times reaching beyond the NAAQS safe standards. With recent trends in surface ozone concentrations as monitored by CPCB via Continuous Ambient Air Quality Monitoring Stations network, it has been observed that Ozone levels in Delhi were quite high in days of high temperature conditions. Therefore, in this research we propose to study the variations in surface ozone concentrations in 5 distinct districts of Delhi i.e., North Delhi, South Delhi, New Delhi, West Delhi and South East Delhi over a period of 1 year starting from May 2021 to May 2022.

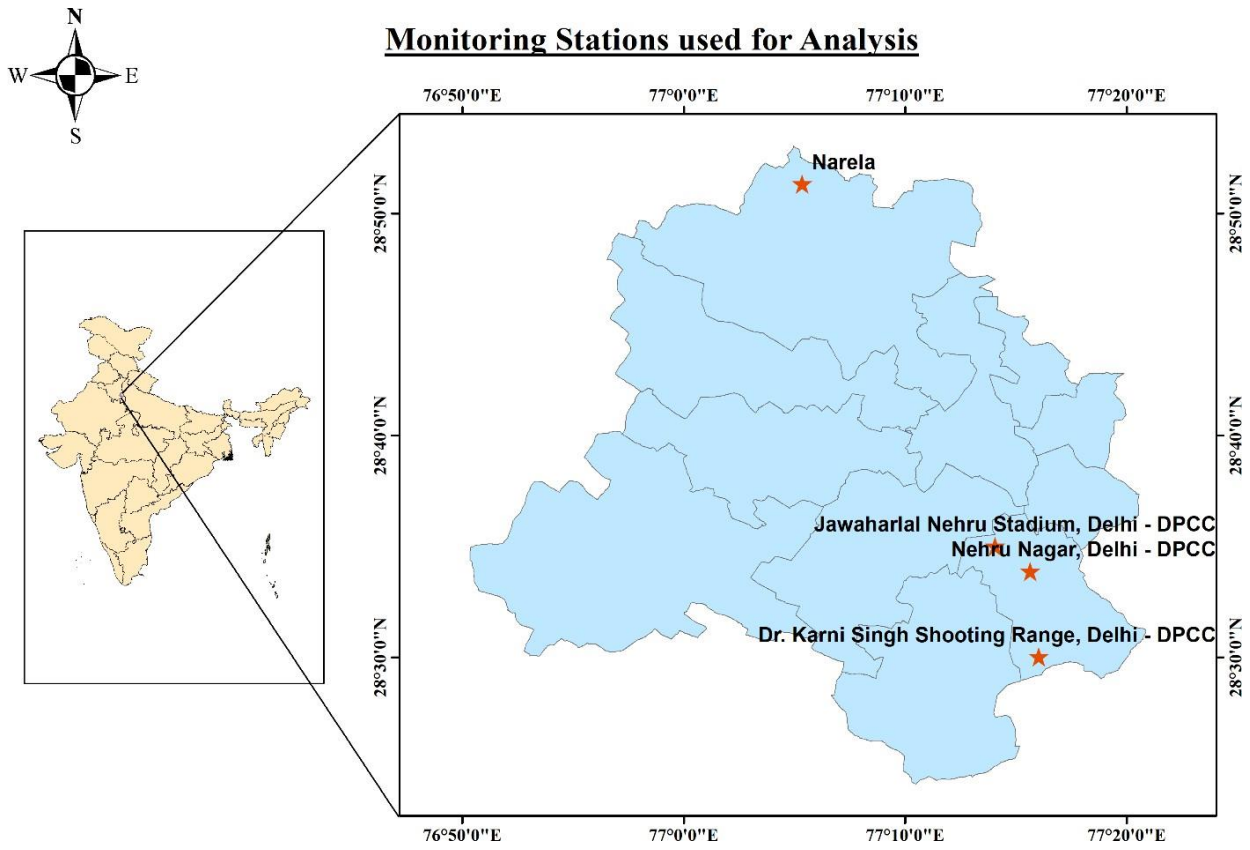

Figure 3.1: Study area with locations of 4 monitoring stations used for analysis

3.2 DATA COLLECTION AND ANALYSIS

The surface ozone concentration is monitored by Central Pollution Control Board for 15 -minute duration across 38 monitoring stations in Delhi. Out of 38 stations 4 monitoring stations i.e., Narela, Nehru Nagar, JLN Stadium, Dr. Karni Shooting Range, each for 5 district North Delhi, South Delhi, New Delhi, West Delhi and South East Delhi respectively. The hourly data for Ozone, Ambient Temperature, Relative Humidity, Particulate Matter (PM2.5, PM10), Sulphur Dioxide (SO_2), Nitric Oxide (NO), Nitrogen Dioxide (NO_2), NO_x, Carbon Monoxide (CO) and Wind Speed has been downloaded from https://app.cpcbccr.com/ccr/#/caaqm-dashboard-all/caaqm-landing for a duration one year from 1st May 2021 to 19th May 2022.

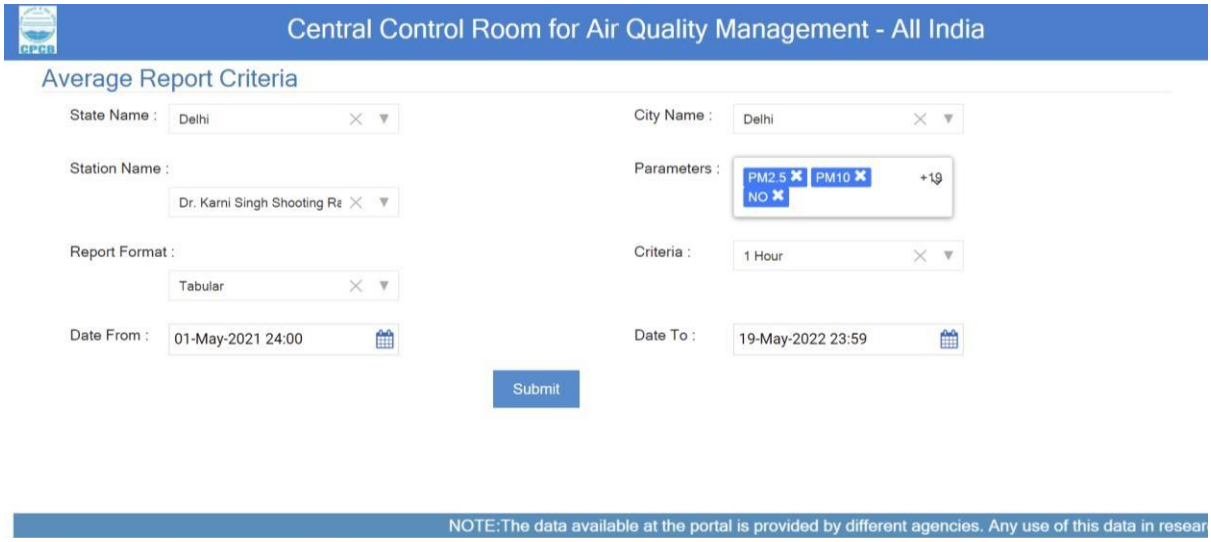

Figure 3.2: CPCB CCR website for downloading the continuous ambient air quality data.

Chapter 4

RESULTS AND DISCUSSIONS

4.1 Hourly Variations in Ozone concentrations

The hourly ozone concentrations for the 4 locations over last year ranged from 0.1 to 199.9 μgm^{-3}, 0.72 to 198.8 μgm^{-3}, 0.5 to 199.9 μgm^{-3}, 0.1 to 196.85 μgm^{-3} for Jawahar Lal Nehru Stadium, Dr. Karni Singh Shooting Range, Nehru Nagar and Narela respectively. For JLN stadium, May- 22 saw the maximum hourly ozone concentration of 199.9 μgm^{-3} while the lowest was 0.1 μgm^{-3} for August 2022. For Dr. Karni Singh Shooting Range minimum concentration was in May 2022(0.72 μgm^{-3}) and the maximum hourly value was 198.8 μgm^{-3} observed in May 2021. Whereas, atNehru Nagar, the maximum and minimum extremities were observed in October 2021, April 2022 (maximum – 199.5 μgm^{-3}) and August 2021 (minimum – 0.1 μgm^{-3}) respectively. Narela observed the maximum hourly concentration in November 2021 (198.65 μgm^{-3}) and the minimum in January 2022 (0.1 μgm^{-3}). The hourly concentrations of ozone were found to be above the CPCB standards of 180 μgm^{-3} per hour for both residential and sensitive zones. Out of more than 9000 hourly observations, 160 times the ozone level exceeded the hourly safe limit at JLN stadium andall the times the violation was observed for afternoon hours. Exceeding values were observed for 11:00 to 16:00 hours at JLN stadium. While the concentration of ozone exceeded for 195 hours in1 year for Dr. Karni Singh Shooting Range, 222 hours for Nehru Nagar, and for 56 hours for Narela. The maximum and minimum hourly concentrations observed for all locations are listed intables below (Table 4.1 to 4.4).

Table 4.1: Variations in ozone concentrations from May 2021 to May 2022 (in μgm^{-3}) for JLN stadium

S. No.	Months	Monthly Mean	Maximum Hourly Concentration	Minimum Hourly Concentration
1	May-21	39.407	156.400	0.480
2	Jun-21	29.919	151.880	0.800
3	Jul-21	18.004	154.150	0.650
4	Aug-21	10.525	120.200	0.100
5	Sep-21	16.159	198.800	0.400
6	Oct-21	38.877	197.100	4.300
7	Nov-21	34.907	187.550	0.300
8	Dec-21	25.811	156.380	0.200
9	Jan-22	25.291	142.430	0.300
10	Feb-22	41.813	174.900	0.300
11	Mar-22	53.819	197.800	0.200
12	Apr-22	68.022	199.700	0.700
13	May-22	72.976	199.900	3.050

Table 4.2: Variations in ozone concentrations from May 2021 to May 2022 (in μgm^{-3}) for Dr. Karni Singh Shooting Range

S. No.	Months	Monthly Mean	Maximum Hourly Concentration	Minimum Hourly Concentration
1	May-21	84.089	198.800	5.500
2	Jun-21	72.582	195.950	4.420
3	Jul-21	45.281	185.800	3.550
4	Aug-21	29.381	71.300	0.900
5	Sep-21	29.771	73.500	3.670
6	Oct-21	45.059	190.400	2.170
7	Nov-21	58.847	196.200	2.720
8	Dec-21	43.456	187.720	2.830
9	Jan-22	37.390	153.600	4.580
10	Feb-22	60.166	192.700	4.880
11	Mar-22	62.937	191.600	2.050
12	Apr-22	70.034	195.400	0.970
13	May-22	96.195	195.900	0.720

Table 4.3: Monthly variations in ozone concentrations from May 2021 to May 2022 (in μgm^{-3}) for Nehru Nagar:

S. No.	Months	Monthly Mean	Maximum Hourly Concentration	Minimum Hourly Concentration
1	May-21	71.104	199.500	2.250
2	Jun-21	63.206	197.800	0.970
3	Jul-21	33.461	184.200	0.500
4	Aug-21	21.738	173.200	0.100
5	Sep-21	20.228	189.930	1.530
6	Oct-21	38.296	199.500	2.250
7	Nov-21	31.033	196.900	1.900
8	Dec-21	22.415	161.320	2.920
9	Jan-22	15.500	123.700	1.270
10	Feb-22	41.989	195.300	1.520
11	Mar-22	54.937	197.500	0.750
12	Apr-22	63.605	199.900	0.500
13	May-22	79.679	199.500	0.300

Table 4.4: Monthly variations in ozone concentrations from May 2021 to May 2022 (in μgm^{-3}) for Narela:

S. No.	Months	Monthly Mean	Maximum Hourly Concentration	Minimum Hourly Concentration
1	May-21	60.146	186.450	1.250
2	Jun-21	59.772	173.650	3.100
3	Jul-21	55.854	149.700	10.900
4	Aug-21	42.800	118.670	12.500
5	Sep-21	45.468	132.930	15.620
6	Oct-21	41.309	144.100	2.700
7	Nov-21	43.682	198.650	0.680
8	Dec-21	29.300	139.820	1.050
9	Jan-22	22.361	126.550	0.100
10	Feb-22	41.821	171.650	0.400
11	Mar-22	53.313	196.250	2.270
12	Apr-22	63.658	197.050	0.170
13	May-22	72.115	196.800	0.200

4.2 Monthly Variations in Ozone Concentrations

The monthly variations in ozone concentrations are depicted in figure 4.1 to 4.4 and tabulated in Table 4.1 to 4.4. As observed, the monthly means were maximum for the months of April, May

and June with maximum in May 2022 for all the locations. The minimum monthly observations were in January 2022 for Narela and Nehru Nagar, while at JLN stadium and Dr. Karni Singh Shooting Range the minimum values were in August 2021. The highest monthly average for among all locations was observed for Dr. Karni Singh shooting range in May 2022 at 96.125 μgm^{-3}.

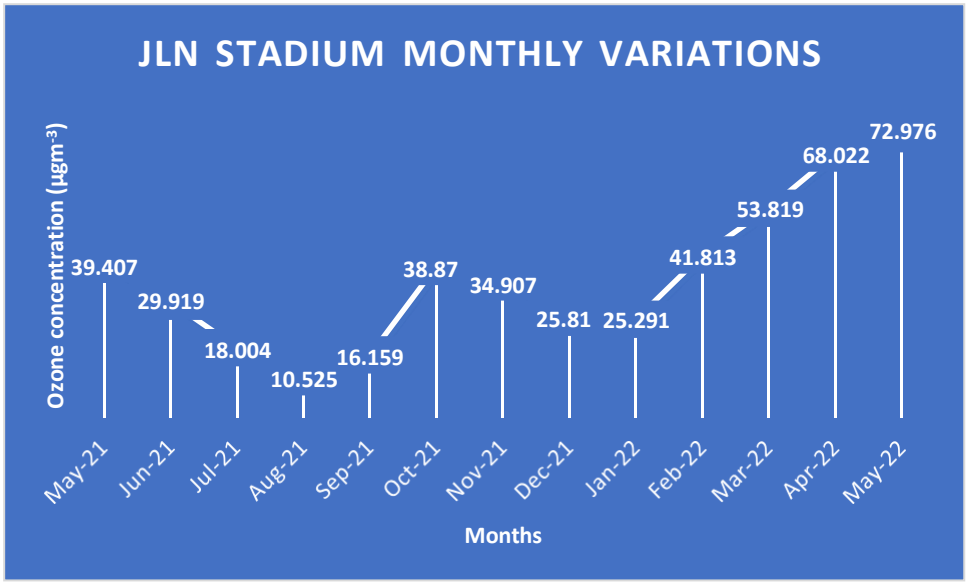

Figure 4.1: Monthly variations in ozone concentrations (in μgm^{-3}) at JLN stadium

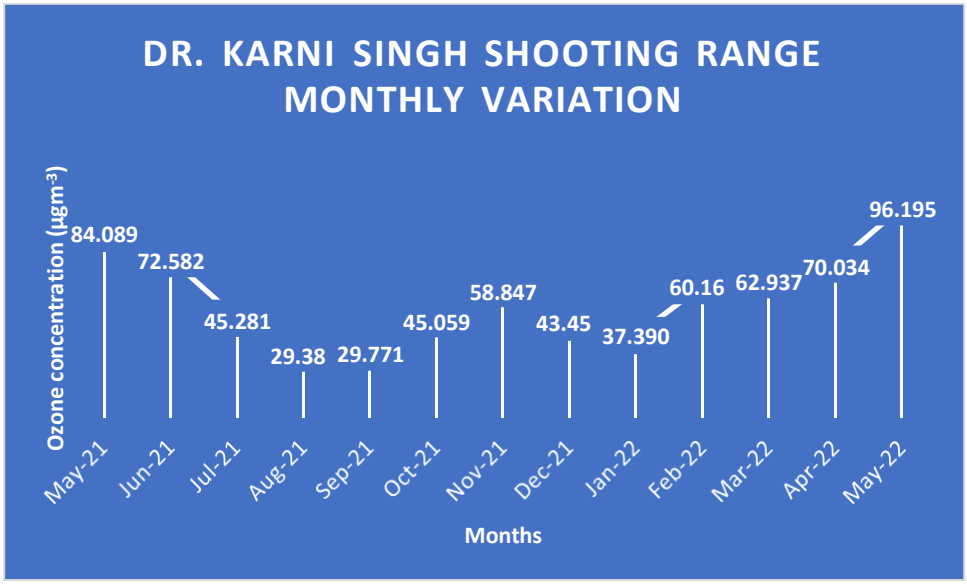

Figure 4.2: Monthly variations in ozone concentrations (in μgm^{-3}) at Dr. Karni Singh Shooting Range

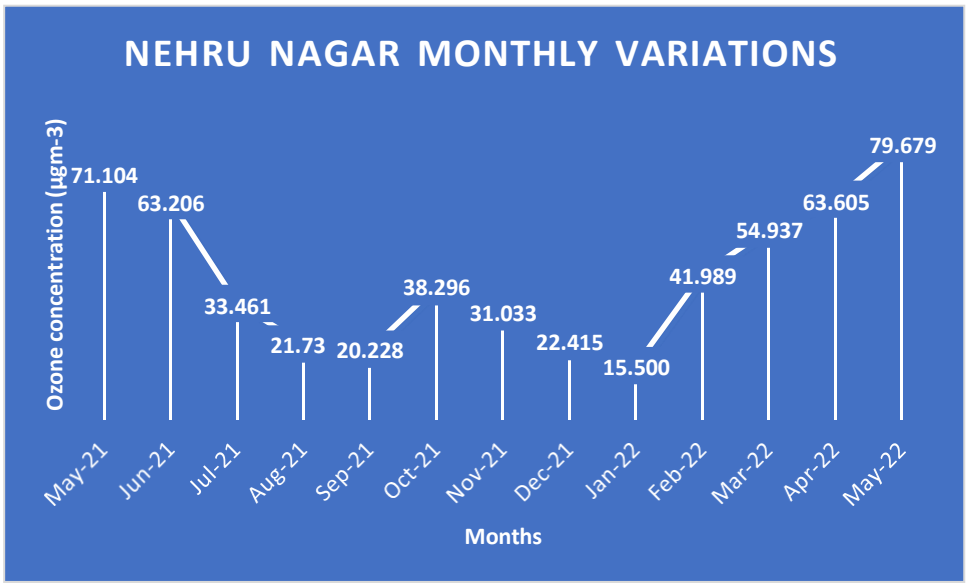

Figure 4.3: Monthly variations in ozone concentrations (in μgm^{-3}) at Nehru Nagar

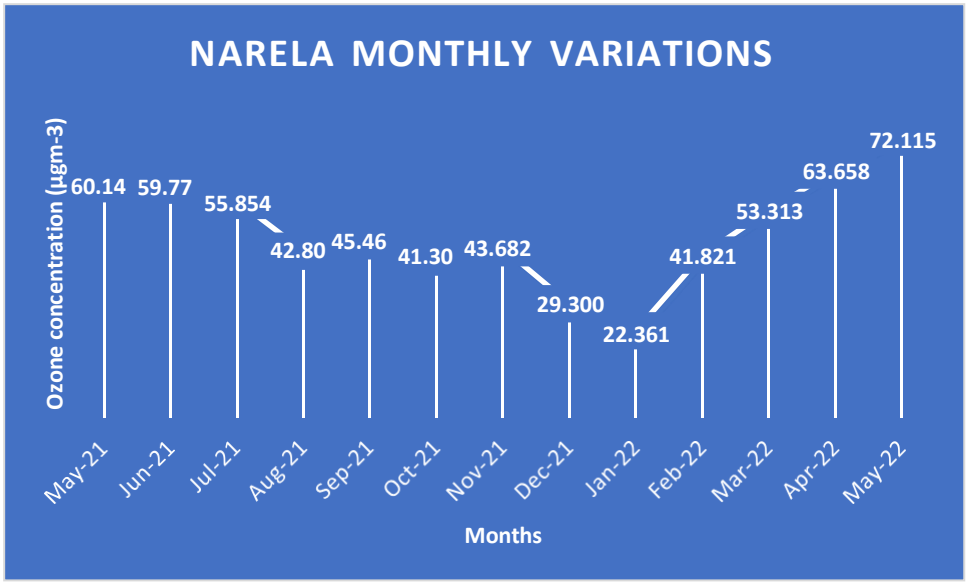

Figure 4.4: Monthly variations in ozone concentrations (in μgm^{-3}) at Narela

4.3 Seasonal Variations in Ozone Concentrations

The seasonal variations in ozone concentrations are depicted in figures 4.5 to 4.8 and mean values are tabulated in Tables 4.5 to 4.8. It is observed for all locations, though the extreme values were observed for all seasons with values reaching as high as 199.9 μgm^{-3}, the average concentrations are maximum in summers. This may be due to the impact of increased temperature in summers and subsequently the heatwave situations which make ozone concentrations even higher. With an

increase in solar radiations, the reactions leading to formation of ozone get catalyzed thereby increasing ozone. More details on this are discussed in later sections.

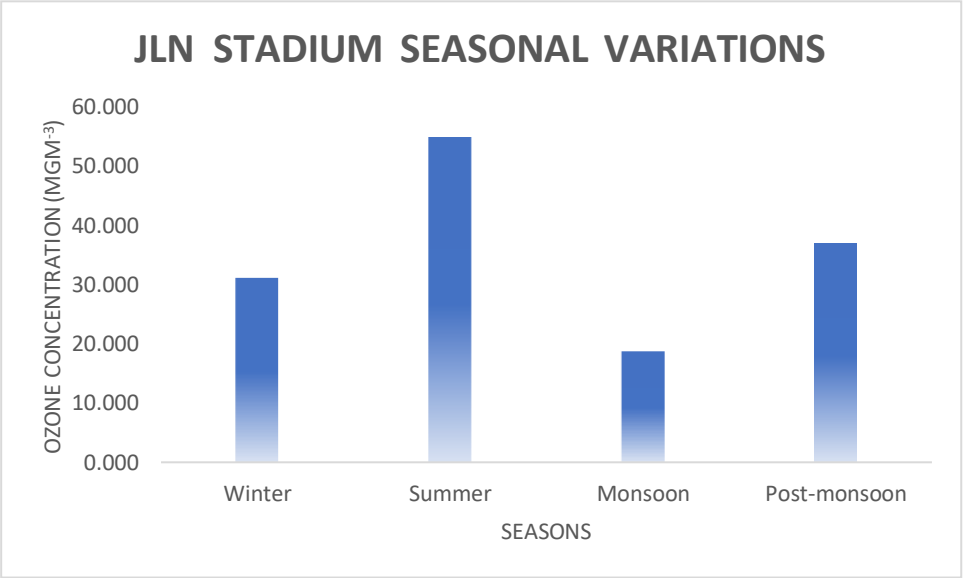

Figure 4.5: Seasonal variations in ozone concentrations (in μgm^{-3}) at JLN stadium

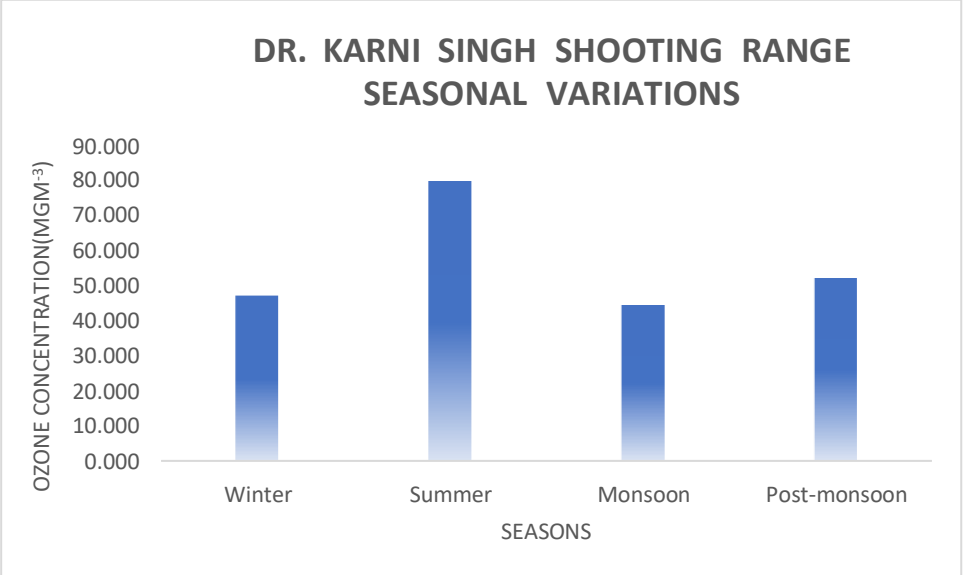

Figure 4.6: Seasonal variations in ozone concentrations (in μgm^{-3}) at Dr. Karni Singh Shooting Range

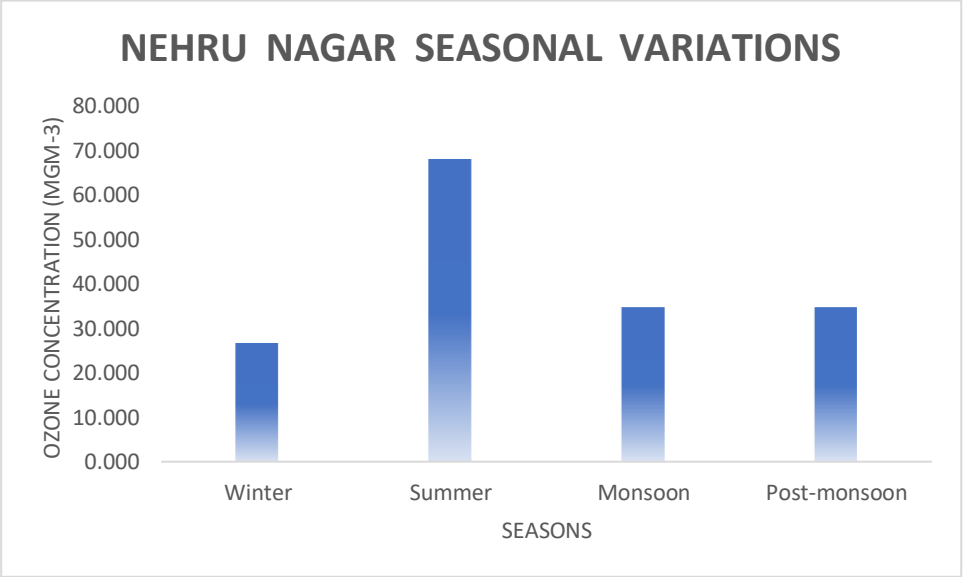

Figure 4.7: Seasonal variations in ozone concentrations (in μgm^{-3}) at Nehru Nagar

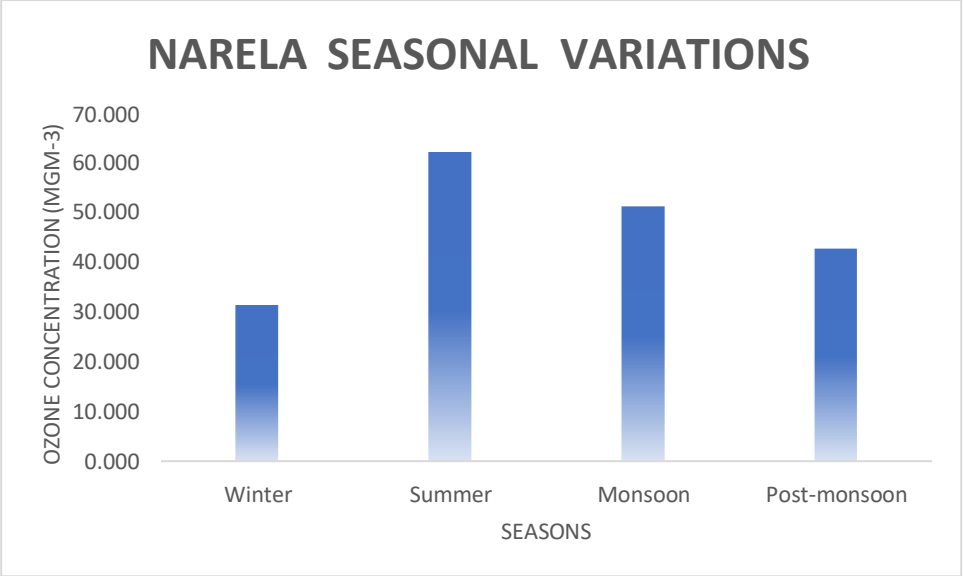

Figure 4.8: Seasonal variations in ozone concentrations (in μgm^{-3}) at Narela

Table 4.5: Seasonal variations in ozone concentrations from May 2021 to May 2022 (in μgm^{-3}) for JLN Area:

Seasonal Variations	**Mean**	**Maximum**	**Minimum**
Winter	30.972	174.900	0.200
Summer	54.726	199.900	0.200
Monsoon	18.652	198.800	0.100
Post-monsoon	36.892	197.100	0.300

Table 4.6: Seasonal variations in ozone concentrations from May 2021 to May 2022 (in μgm^{-3}) for Karni Area:

Seasonal Variations	**Mean**	**Maximum**	**Minimum**
Winter	47.004	192.700	2.830
Summer	79.469	198.800	0.720
Monsoon	44.254	195.950	0.900
Post-monsoon	51.953	196.200	2.170

Table 4.7: Seasonal variations in ozone concentrations from May 2021 to May 2022 (in μgm^{-3}) for Nehru Nagar Area:

Seasonal Variations	**Mean**	**Maximum**	**Minimum**
Winter	26.635	195.300	1.270
Summer	68.086	199.900	0.300
Monsoon	34.658	197.800	0.100
Post-monsoon	34.665	199.500	1.900

Table 4.8: Seasonal variations in ozone concentrations from May 2021 to May 2022 (in μgm^{-3}) for Narela Area:

Seasonal	**Seasonal** Mean	**Maximum**	**Minimum**
Winter	31.161	171.650	0.100
Summer	61.876	197.050	0.170
Monsoon	50.974	173.650	3.100
Post-monsoon	42.496	198.650	0.680

4.4 Spearman Correlation analysis (Bivariate level)

Spearman correlation test was used to assess the size and direction of the linear connection among ozone with meteorological variables to calculate bivariate correlation coefficient (r). Table 4.9, 4.10, 4.11, 4.12 and Figure 4.9 to 4.12 shows all the r values calculated for all the selected monitoring sites in which it was observed that ozone and meteorological variables r values are varying which can be determined as site wise: -

1. As shown in correlation maps, during the selected time period in Jawaharlal Nehru surface level ozone (O_3) shown significant moderate positive association with temperature ($r = 0.342$, $p < 0.05$), and wind speed ($r = 0.341$, $p < 0.05$) which indicate that the rise in temperature and wind speed will positively impact the concentration of ozone.

Additionally, it shown weak significant moderate association with $PM_{2.5}$ (r = - 0.144, p < 0.05), PM_{10} ((r = - 0.037, p < 0.05), SO_2 (r = - 0.034, p < 0.05) and moderate negative significant association with NO (r = - 0.532, p < 0.05), NO_2 (r = - 0.382, p < 0.05), NOx (r = - 0.555, p < 0.05), and relative humidity (r = - 0.672, p < 0.05).

2. As portrayed in correlation maps, during the selected time period in Dr. Karni Singh Shooting Range surface level ozone (O_3) shown significant moderate positive association with temperature (r = 0.306, p < 0.05), SO2 (r = 0.232, p < 0.05) and wind speed (r = 0.520, p < 0.05) which indicate that the rise in temperature, sulfur di oxide and wind speed will positively impact the concentration of ozone. Additionally, it shown weak significant moderate association with $PM_{2.5}$ (r = - 0.156, p < 0.05), PM_{10} (r = - 0.105, p < 0.05) and strong significant negative association with NO (r = - 0.705, p < 0.05), NO2 (r = - 0.425, p < 0.05), NOx (r = - 0.552, p < 0.05), CO (r = - 0.432, p < 0.05), and relative humidity (r = - 0.610, p < 0.05).

Table 4.9: Correlation matrix (Spearman) for JLN Stadium

Variables	PM2.5	PM10	NO	NO2	NOx	SO2	CO	Ozone	AT	RH	WS
PM2.5	**1**	**0.859**	**0.603**	**0.377**	**0.556**	**0.451**	**0.670**	**-0.144**	**-0.538**	**0.257**	**0.103**
PM10	**0.859**	**1**	**0.513**	**0.394**	**0.517**	**0.463**	**0.602**	**-0.037**	**-0.301**	**-0.025**	**0.170**
NO	**0.603**	**0.513**	**1**	**0.560**	**0.847**	**0.402**	**0.793**	**-0.542**	**-0.532**	**0.475**	**-0.137**
NO2	**0.377**	**0.394**	**0.560**	**1**	**0.852**	**0.257**	**0.444**	**-0.382**	**-0.217**	**0.190**	**-0.197**
NOx	**0.556**	**0.517**	**0.847**	**0.852**	**1**	**0.373**	**0.689**	**-0.555**	**-0.431**	**0.419**	**-0.239**
SO2	**0.451**	**0.463**	**0.402**	**0.257**	**0.373**	**1**	**0.445**	**-0.034**	**-0.165**	-0.009	0.020
CO	**0.670**	**0.602**	**0.793**	**0.444**	**0.689**	**0.445**	**1**	**-0.329**	**-0.445**	**0.339**	**-0.070**
Ozone	**-0.144**	**-0.037**	**-0.542**	**-0.382**	**-0.555**	**-0.034**	**-0.329**	**1**	**0.342**	**-0.672**	**0.341**
AT	**-0.538**	**-0.301**	**-0.532**	**-0.217**	**-0.431**	**-0.165**	**-0.445**	**0.342**	**1**	**-0.568**	**-0.130**
RH	**0.257**	**-0.025**	**0.475**	**0.190**	**0.419**	-0.009	**0.339**	**-0.672**	**-0.568**	**1**	**-0.326**
WS	**0.103**	**0.170**	**-0.137**	**-0.197**	**-0.239**	0.020	**-0.070**	**0.341**	**-0.130**	**-0.326**	**1**

Table 4.10: Correlation matrix (Spearman) for Dr. Karni Singh Shooting Range

Variables	PM2.5	PM10	NO	NO2	NOx	SO2	CO	Ozone	RH	WS	AT
PM2.5	1	0.889	0.319	0.643	0.572	0.399	0.605	-0.156	0.025	-0.227	-0.570
PM10	0.889	1	0.253	0.606	0.518	0.500	0.595	-0.105	-0.212	-0.163	-0.351
NO	0.319	0.253	1	0.734	0.869	-0.204	0.545	-0.705	0.488	-0.468	-0.365
NO2	0.643	0.606	0.734	1	0.965	0.175	0.635	-0.425	0.118	-0.412	-0.509
NOx	0.572	0.518	0.869	0.965	1	0.056	0.654	-0.552	0.267	-0.475	-0.499
SO2	0.399	0.500	-0.204	0.175	0.056	1	0.169	0.232	-0.572	0.052	-0.109
CO	0.605	0.595	0.545	0.635	0.654	0.169	1	-0.432	0.156	-0.466	-0.232
Ozone	-0.156	-0.105	-0.705	-0.425	-0.552	0.232	-0.432	1	-0.610	0.520	0.306
RH	0.025	-0.212	0.488	0.118	0.267	-0.572	0.156	-0.610	1	-0.359	-0.405
WS	-0.227	-0.163	-0.468	-0.412	-0.475	0.052	-0.466	0.520	-0.359	1	0.197
AT	-0.570	-0.351	-0.365	-0.509	-0.499	-0.109	-0.232	0.306	-0.405	0.197	1

Table 4.11: Correlation matrix (Spearman) for Nehru Nagar

Variables	PM2.5	PM10	NO	NO2	NOx	SO2	CO	Ozone	RH	WS	AT
PM2.5	1	0.900	0.509	0.661	0.670	0.439	0.518	-0.304	0.098	-0.251	-0.606
PM10	0.900	1	0.449	0.633	0.615	0.531	0.417	-0.216	-0.128	-0.190	-0.384
NO	0.509	0.449	1	0.653	0.868	0.135	0.463	-0.691	0.423	-0.190	-0.545
NO2	0.661	0.633	0.653	1	0.905	0.312	0.484	-0.485	0.122	-0.289	-0.489
NOx	0.670	0.615	0.868	0.905	1	0.255	0.523	-0.625	0.312	-0.276	-0.587
SO2	0.439	0.531	0.135	0.312	0.255	1	0.231	0.091	-0.417	0.102	-0.037
CO	0.518	0.417	0.463	0.484	0.523	0.231	1	-0.247	0.256	-0.241	-0.491
Ozone	-0.304	-0.216	-0.691	-0.485	-0.625	0.091	-0.247	1	-0.525	0.061	0.518
RH	0.098	-0.128	0.423	0.122	0.312	-0.417	0.256	-0.525	1	-0.170	-0.625
WS	-0.251	-0.190	-0.190	-0.289	-0.276	0.102	-0.241	0.061	-0.170	1	0.222
AT	-0.606	-0.384	-0.545	-0.489	-0.587	-0.037	-0.491	0.518	-0.625	0.222	1

Table 4.11: Correlation matrix (Spearman) for Narela

Variables	PM2.5	PM10	NO	NO2	NOx	SO2	CO	Ozone	RH	WS	AT
PM2.5	1	0.865	0.415	0.571	0.560	0.547	0.100	-0.416	0.287	-0.237	-0.554
PM10	0.865	1	0.348	0.529	0.494	0.614	0.136	-0.286	0.029	-0.197	-0.257
NO	0.415	0.348	1	0.674	0.838	0.116	0.257	-0.647	0.405	-0.203	-0.412
NO2	0.571	0.529	0.674	1	0.945	0.306	0.298	-0.569	0.311	-0.304	-0.448
NOx	0.560	0.494	0.838	0.945	1	0.225	0.321	-0.654	0.409	-0.290	-0.498
SO2	0.547	0.614	0.116	0.306	0.225	1	0.083	0.033	-0.306	-0.110	0.055
CO	0.100	0.136	0.257	0.298	0.321	0.083	1	-0.263	0.157	-0.005	-0.029
Ozone	-0.416	-0.286	-0.647	-0.569	-0.654	0.033	-0.263	1	-0.670	0.107	0.666
RH	0.287	0.029	0.405	0.311	0.409	-0.306	0.157	-0.670	1	-0.073	-0.752
WS	-0.237	-0.197	-0.203	-0.304	-0.290	-0.110	-0.005	0.107	-0.073	1	0.168
AT	-0.554	-0.257	-0.412	-0.448	-0.498	0.055	-0.029	0.666	-0.752	0.168	1

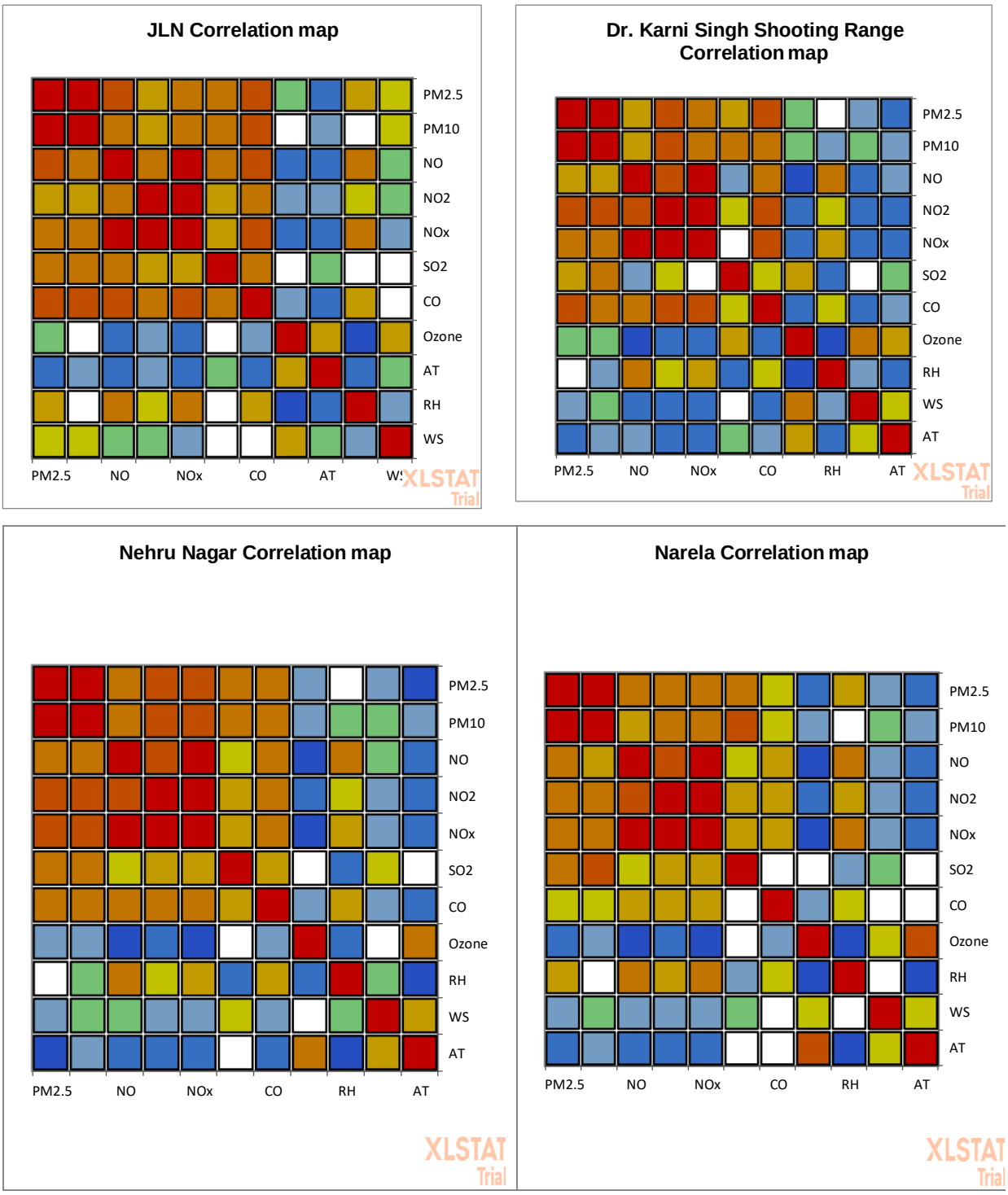

Figure 4.9: Correlation maps generated from Spearman Correlation Analysis

3. As indicated in correlation maps, during the selected time period in Nehru Nagar surface level ozone (O_3) shown significant strong positive association with temperature (r = 0.518, $p < 0.05$), and weak association with SO_2 (r = 0.0.091, $p < 0.05$) and wind speed (r = 0.0.061, $p < 0.05$) which indicate that the rise in temperature, sulfur di oxide and wind

speed will positively impact the concentration of ozone. Additionally, it shown weak significant moderate association with $PM_{2.5}$ (r = - 0.304, $p < 0.05$), PM_{10} (r = - 0.216, $p < 0.05$) and strong significant negative association with NO (r = - 0.691, $p < 0.05$), NO2 (r = - 0.485, $p < 0.05$), NOx (r = - 0.625, $p < 0.05$), CO (r = - 0.247, $p < 0.05$), and relative humidity (r = - 0.525, $p < 0.05$).

4. As shown in correlation maps, during the selected time period in Narela surface level ozone (O_3) shown significant strong positive association with temperature (r = 0.666, $p < 0.05$), and weak association with SO_2 (r = 0.033, $p < 0.05$) and wind speed (r = 0.107, $p < 0.05$) which indicate that the rise in temperature, sulfur di oxide and wind speed will positively impact the concentration of ozone. Additionally, it shown significant moderate association with $PM_{2.5}$ (r = - 0.416, $p < 0.05$), PM_{10} (r = - 0.286, $p < 0.05$) and strong significant negative association with NO (r = - 0.647, $p < 0.05$), NO_2 (r = - 0.569, $p < 0.05$), NOx (r = - 0.654, $p < 0.05$), CO (r = - 0.263, $p < 0.05$), and relative humidity (r = - 0.670, $p < 0.05$).

   All the above appeared results are indicated that in all the regions ozone is strongly associated with temperature, SO_2, and wind speed which further justifying the theory that ozone is impacted by the increase in temperature. Through scatter graphs the association among both are displayed in figure for all study areas. Although, the relationship was assessed at bivariate level which has the drawback of not considering the presence or effect of other independent variables between the two being investigated. So, in our next step to test our hypothesis by tackling this error the dataset will be analyzed at multivariate level using multiple linear regression.

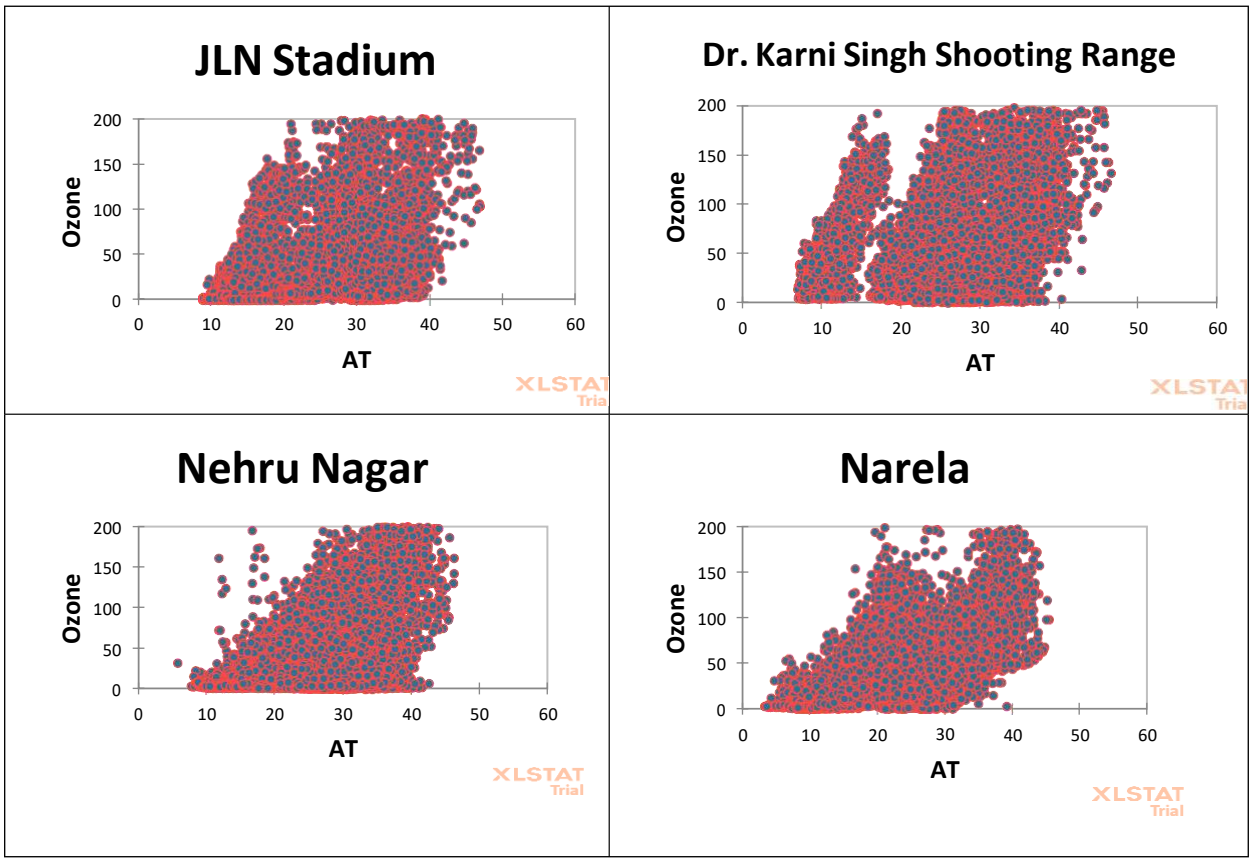

Figure 4.10: Scatter plots representing dependence of Ozone on Atmospheric Temperature

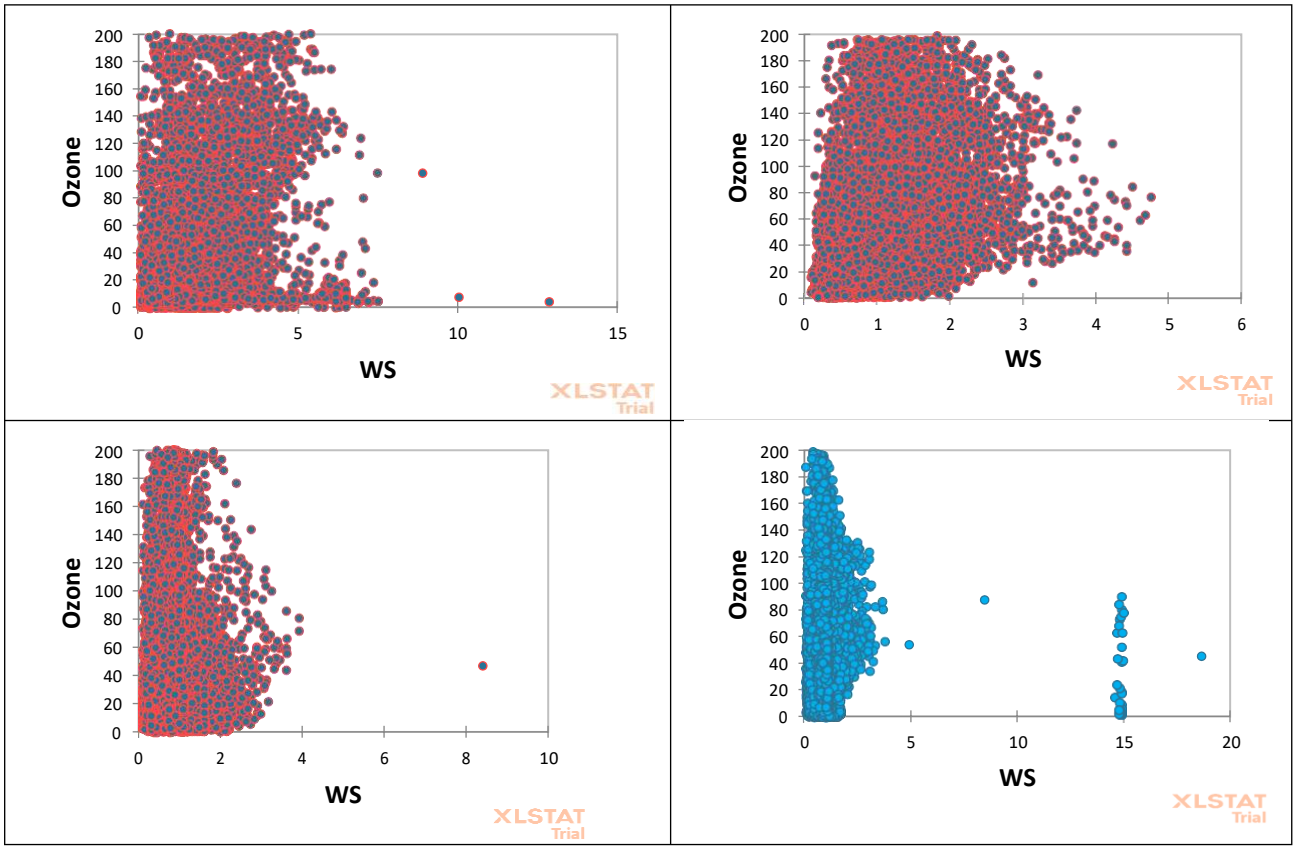

Figure 4.11: Scatter plots representing dependence of Ozone on Wind Speed

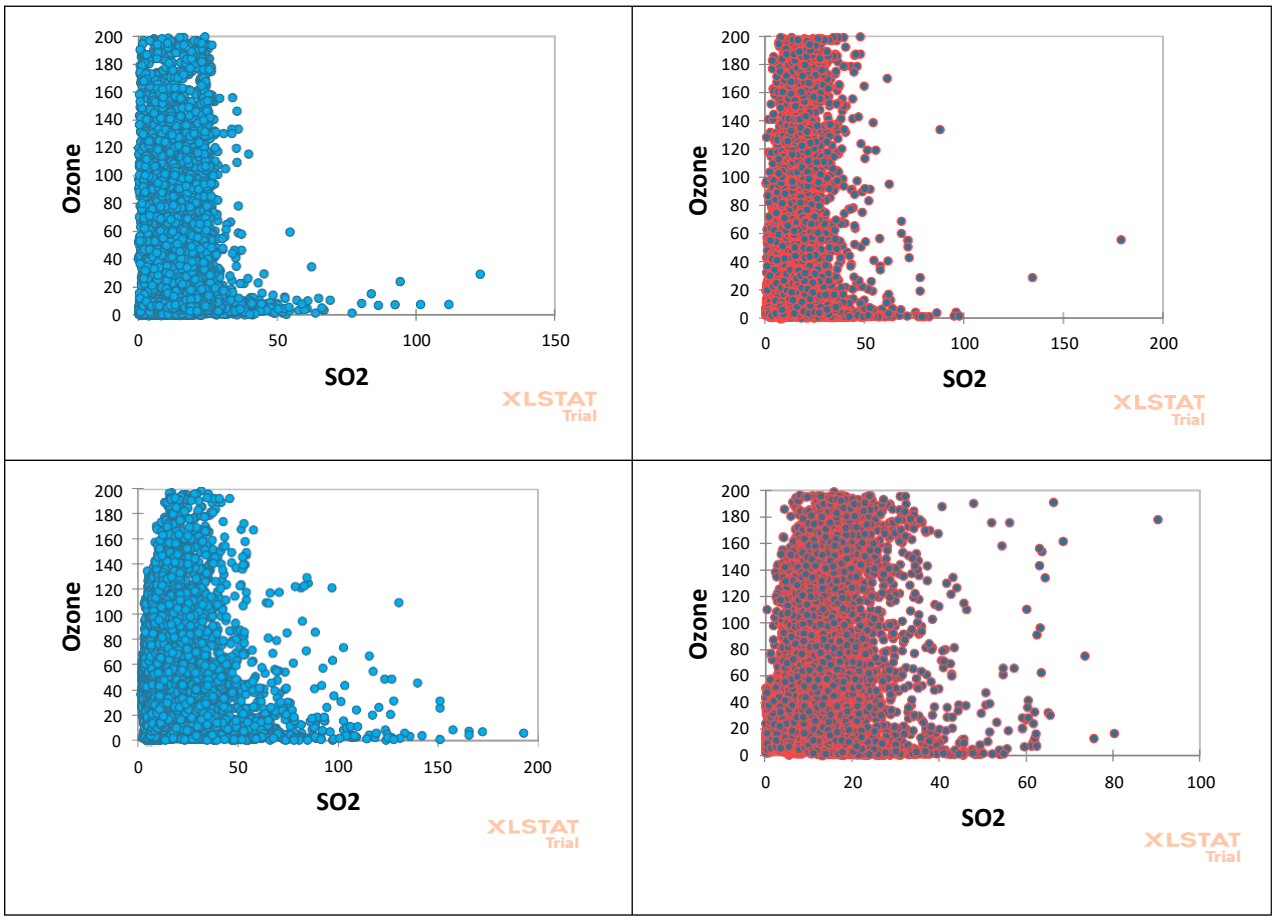

Figure 4.12: Scatter plots representing dependence of Ozone on SO_2

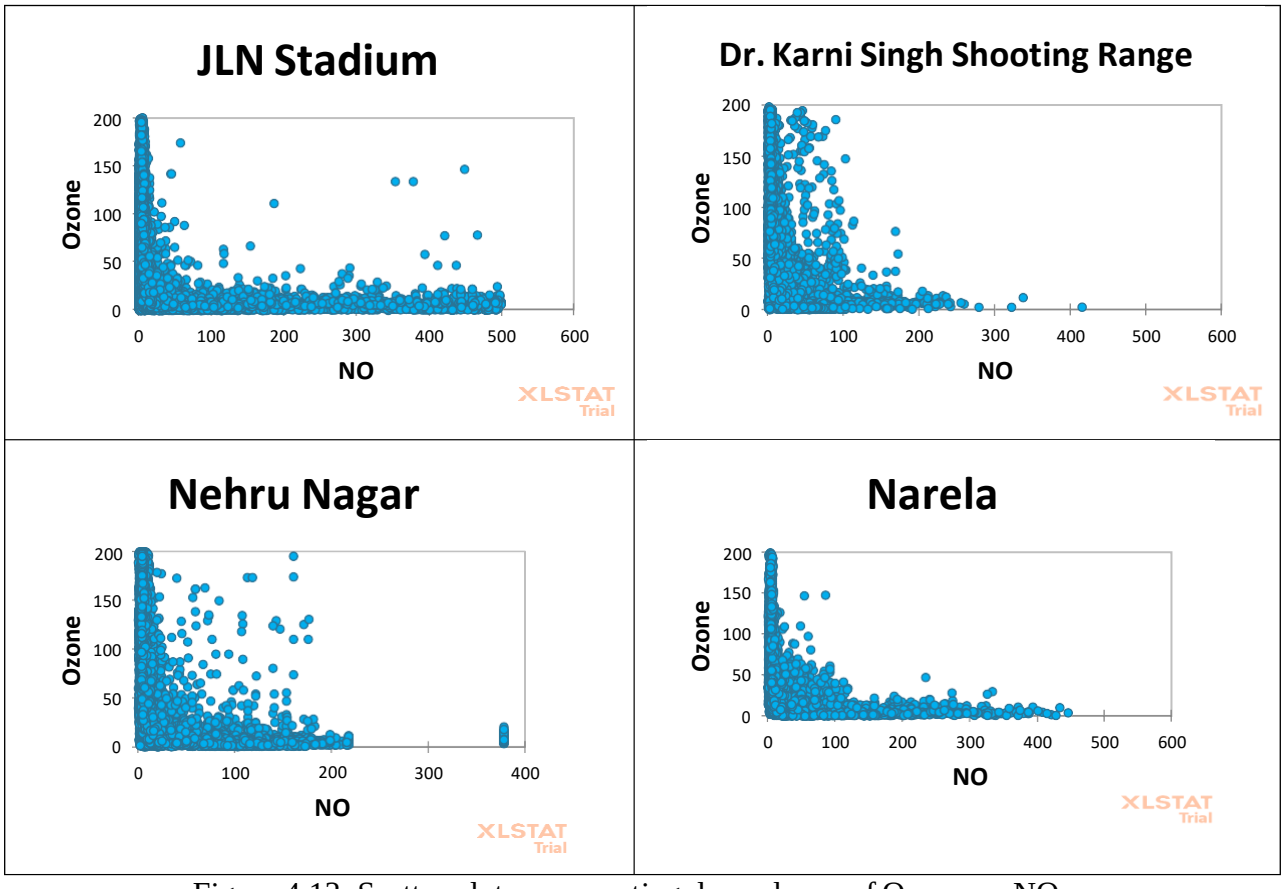

Figure 4.13: Scatter plots representing dependence of Ozone on NO

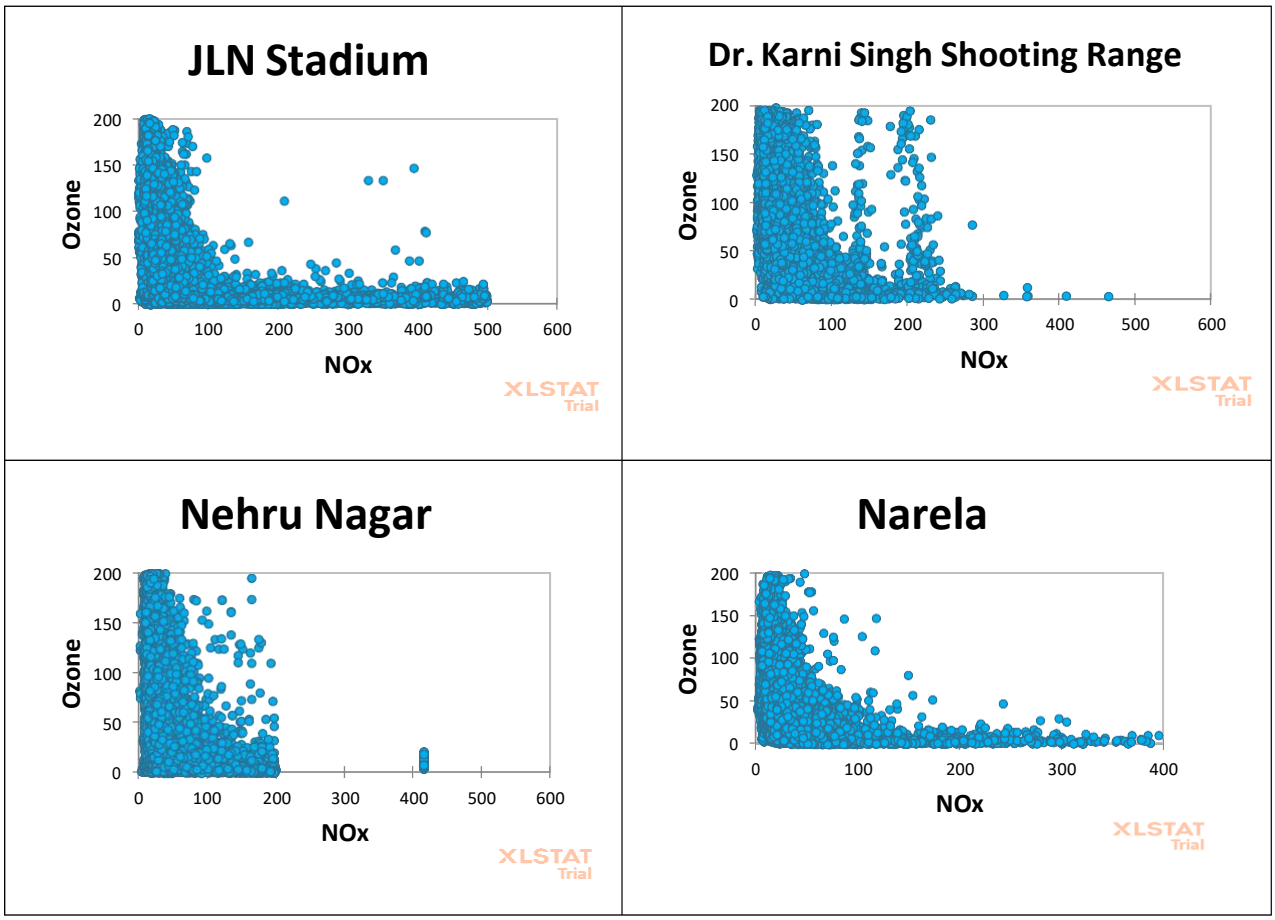

Figure 4.14: Scatter plots representing dependence of Ozone on NO_x

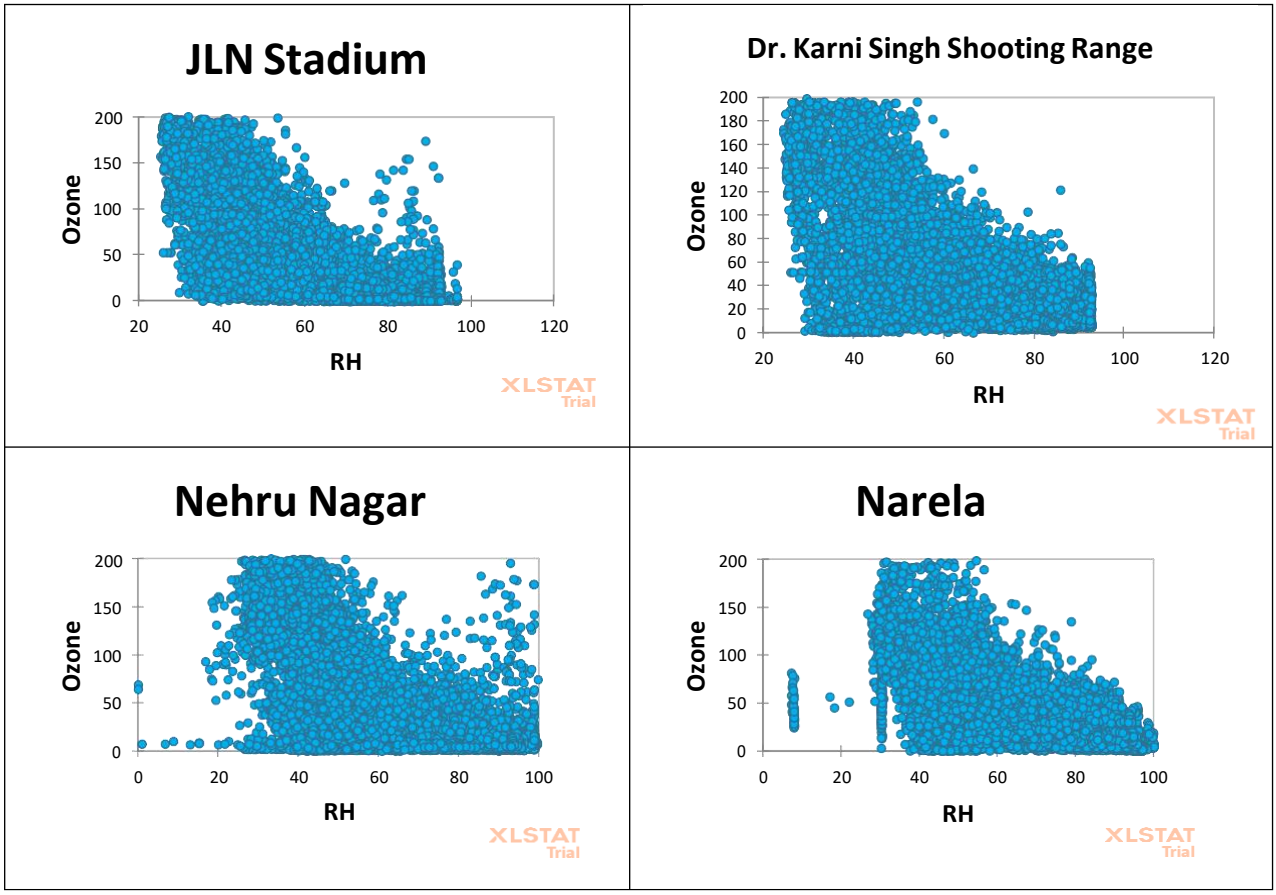

Figure 4.15: Scatter plots representing dependence of Ozone on Relative Humidity

4.5 Multiple Linear Regression

The stepwise method of multiple linear regression was done using XLSTAT in which surface level ozone is selected as dependent variable. All remaining air pollutants and meteorological variables were selected as independent variables the CI (Confidence Interval) chosen for all these models is 95%. The results came after running the model for each monitoring sites are as follows: -

1. In Jawaharlal Nehru stadium the result shows that 55.1% (or adjusted $R^2 = 0.551$) of the variance in O_3 can be accounted for by the other air pollutants and meteorological parameters, collectively, F (9, 9239) = 1134.385, $p < 0.0001$ as shown in below tables. Looking at the unique individual contributions of the predictors, the results show that $PM_{2.5}$ (β= 0.367, t= 22.8, $p < 0.0001$), NO (β= 0.16, t= 2.4, $p < 0.0001$), SO_2 (β= 0.027, t= 3.3, $p < 0.0001$), CO (β= 0.097, t= 5.8, $p < 0.0001$), and WS (β= 0.082, t= -10.5, $p < 0.048$) were among the most significant ($p < 0.05$) air pollutant and meteorological factors that influenced the incidence of rise in surface ozone level over JLN stadium which are portrayed in equation (1)

$$Ozone=171.936+0.199*PM_{2.5}-7.202E-02*PM_{10}+0.0698*NO-0.375*NO_2-0.127*NOx+0.143*SO_2+3.101*CO + 0.4201*AT-1.734*RH+3.272*WS \quad (1)$$

From the above equation (1) it can be said that with every 1^o celcius rise in atmospheric temperature the surface ozone levels will rise by 0.420. Which further indicates a good positive impact from temperature in the change of ozone levels in JLN area.

Table 4.12: Goodness of fit statistics for JLN Stadium

Observations	9240
Sum of weights	9240
DF	9229
R^2	0.551
Adjusted R^2	0.551
MSE	978.110
RMSE	31.275
MAPE	299.807
DW	0.296

Cp	11.000
AIC	63634.138
SBC	63712.582
PC	0.450
Press	9050991.854
Q^2	0.550

Table 13: Analysis of Variance for JLN Stadium

Source	**DF**	**Sum of squares**	**Mean squares**	**F**	**Pr > F**
Model	10	11095531.027	1109553.103	1134.385	**<0.0001**
Error	9229	9026973.278	978.110		
Corrected Total	9239	20122504.305			

Table 4.14: Model parameters for JLN Stadium

Source	**Value**	**Standard error**	**t**	**Pr > |t|**	**Lower bound (95%)**	**Upper bound (95%)**
$PM_{2.5}$	0.367	0.016	22.840	**<0.0001**	0.336	0.399
PM_{10}	-0.190	0.016	-12.140	**<0.0001**	-0.221	-0.159
NO	0.168	0.067	2.493	**0.013**	0.036	0.300
NO_2	-0.294	0.015	-19.225	**<0.0001**	-0.324	-0.264
NOx	-0.288	0.075	-3.815	**0.000**	-0.435	-0.140
SO_2	0.027	0.008	3.305	**0.001**	0.011	0.043
CO	0.097	0.017	5.797	**<0.0001**	0.064	0.130
AT	-0.072	0.010	-7.105	**<0.0001**	-0.092	-0.052
RH	-0.698	0.011	-63.583	**<0.0001**	-0.720	-0.676
WS	0.085	0.008	10.528	**<0.0001**	0.070	0.101

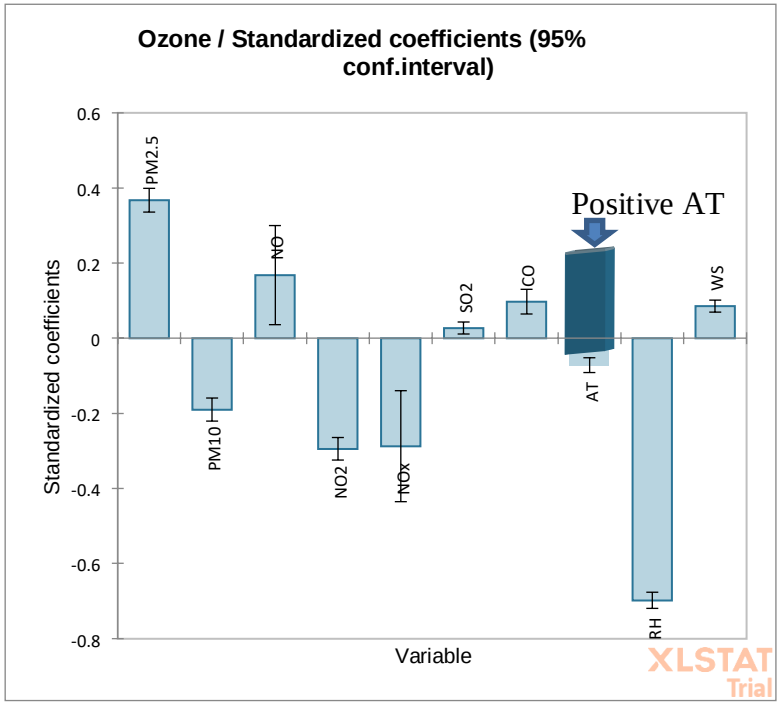

Figure 4.16: β values of each predictor in JLN stadium

2. In Narela the result shows that 56% (or adjusted R^2 = 0.56) of the variance in O_3 can be accounted for by the other air pollutants and meteorological parameters, collectively, F (9, 9230) = 1305.2, p < 0.0001 as shown in below tables. Looking at the unique individual contributions of the predictors, the results show that $PM_{2.5}$ (β= 0.115, t= 17.280, p < 0.0001), and temperature (β= 1.287, t= -22.757, p < 0.0001) were among the most significant (p < 0.05) air pollutant and meteorological factors that influenced the incidence of ozone associated with heat wave in Narela which further are portrayed in Equation (2):

Ozone = 99.168+ 0.115*$PM_{2.5}$- 3.427E-02*PM_{10}- 2.565E-02*NO - 0.353*NO_2- 0.277*SO_2- 5.982*CO-0.928*RH- 1.415*WS + 1.287*AT (2)

From the above equation (2) it can be said that with every 1° celcius rise in atmospheric temperature the surface ozone levels will rise by 1.287. Which further indicates a good positive impact from temperature in the change of ozone levels in Narela.

Table 4.15: Goodness of fit statistics for Narela

Observations	9240
Sum of weights	9240
DF	9230

R^2	0.560
Adjusted R^2	0.560
MSE	668.266
RMSE	25.851
MAPE	136.431
DW	0.223
Cp	10.000
AIC	60113.297
SBC	60184.610
PC	0.441
Press	6182431.134
Q^2	0.559

Table 16: Analysis of Variance for Narela

Source	**DF**	**Sum of squares**	**Mean squares**	**F**	**Pr > F**
Model	9	7850039.670	872226.630	1305.209	**<0.0001**
Error	9230	6168095.785	668.266		
Corrected Total	9239	14018135.454			

Computed against model Y=Mean(Y)

Table 17: Model Parameters for Narela

Source	**Value**	**Standard error**	**t**	**Pr > |t|**	**Lower bound (95%)**	**Upper bound (95%)**
Intercept	99.169	2.813	35.248	**<0.0001**	93.654	104.684
$PM_{2.5}$	0.115	0.007	17.280	**<0.0001**	0.102	0.128
PM_{10}	-0.034	0.004	-8.051	**<0.0001**	-0.043	-0.026
NO	-0.026	0.007	-3.533	**0.000**	-0.040	-0.011
NO_2	-0.353	0.014	-24.870	**<0.0001**	-0.381	-0.325
NOx	0.000	0.000				
SO_2	-0.277	0.022	-12.594	**<0.0001**	-0.320	-0.234
CO	-5.982	0.495	-12.077	**<0.0001**	-6.953	-5.011
RH	-0.928	0.023	-39.712	**<0.0001**	-0.974	-0.883
WS	-1.415	0.237	-5.961	**<0.0001**	-1.880	-0.950
AT	1.287	0.057	22.757	**<0.0001**	1.176	1.398

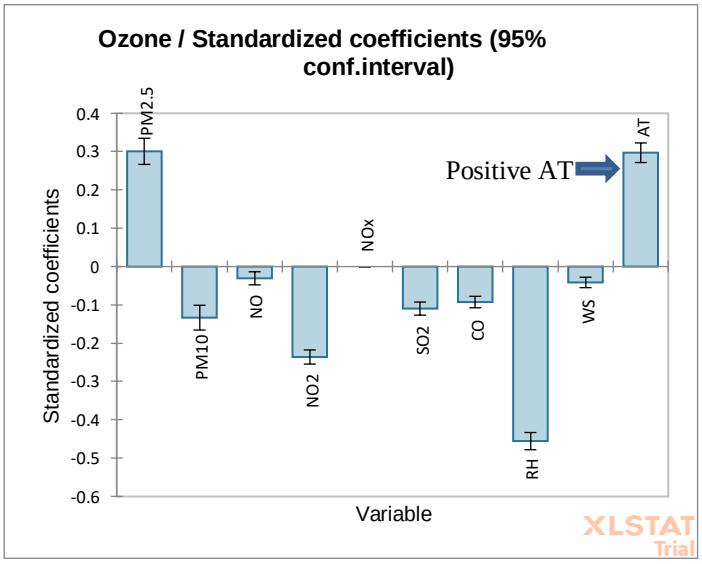

Figure 4.17: β values of each predictor in Narela

3. In Nehru Nagar the result shows that 53.5% (or adjusted $R^2 = 0.56$) of the variance in O_3 can be accounted for by the other air pollutants and meteorological parameters, collectively, F (9, 9183) = 1172.37, $p < 0.0001$ as shown in below tables. Looking at the unique individual contributions of the predictors, the results show that $PM_{2.5}$ (β= 0.056, t= 6.76, $p < 0.0001$), PM_{10} (β= 0.004, t= 0.684, $p < 0.0001$), SO_2 (β= 0.425, t= 9.423, $p < 0.0001$) and temperature (β= 0.72, t= 9.4, $p < 0.0001$) were among the most significant ($p < 0.05$) air pollutant and meteorological factors that influenced the incidence of ozone associated with heat wave in Nehru Nagar which further are portrayed in equation:

$$\boldsymbol{Ozone=132.454+5.617E\text{-}02*PM_{2.5}+4.307E\text{-}03*PM_{10}-0.120*NO-0.483*NO_2+0.425*SO_2+6.250*CO-1.301*RH-10.818*WS+0.7202*AT} \quad \textbf{(3)}$$

From the above equation (3) it can be said that with every 1° Celsius rise in atmospheric temperature the surface ozone levels will rise by 0.720. Which further indicates a good positive impact from temperature in the change of ozone levels in Nehru Nagar.

Table 4.18: Goodness of fit statistics for Nehru Nagar

Observations	9193
Sum of weights	9193

DF	9183
R^2	0.535
Adjusted R^2	0.534
MSE	1183.085
RMSE	34.396
MAPE	280.359
DW	0.547
Cp	10.000
AIC	65058.569
SBC	65129.831
PC	0.466
Press	10892485.504
Q^2	0.533

Table 4.19: Analysis of Variance for Nehru Nagar

Source	DF	Sum of squares	Mean squares	F	Pr > F
Model	9	12483213.650	1387023.739	1172.378	**<0.0001**
Error	9183	10864273.201	1183.085		
Corrected Total	9192	23347486.851			

Computed against model Y=Mean(Y)

Table 4.20: Model Parameters for Nehru Nagar

Source	Value	Standard error	t	Pr > |t|	Lower bound (95%)	Upper bound (95%)
Intercept	132.454	4.080	32.463	**<0.0001**	124.456	140.452
$PM_{2.5}$	0.056	0.008	6.763	**<0.0001**	0.040	0.072
PM_{10}	0.004	0.006	0.684	0.494	-0.008	0.017
NO	-0.120	0.009	-13.680	**<0.0001**	-0.137	-0.103
NO_2	-0.484	0.011	-44.933	**<0.0001**	-0.505	-0.462
NOx	0.000	0.000				
SO_2	0.425	0.045	9.423	**<0.0001**	0.337	0.514
CO	6.250	0.358	17.472	**<0.0001**	5.549	6.952
RH	-1.301	0.029	-44.481	**<0.0001**	-1.359	-1.244
WS	-10.818	0.729	-14.844	**<0.0001**	-12.247	-9.390
AT	0.720	0.076	9.438	**<0.0001**	0.571	0.870

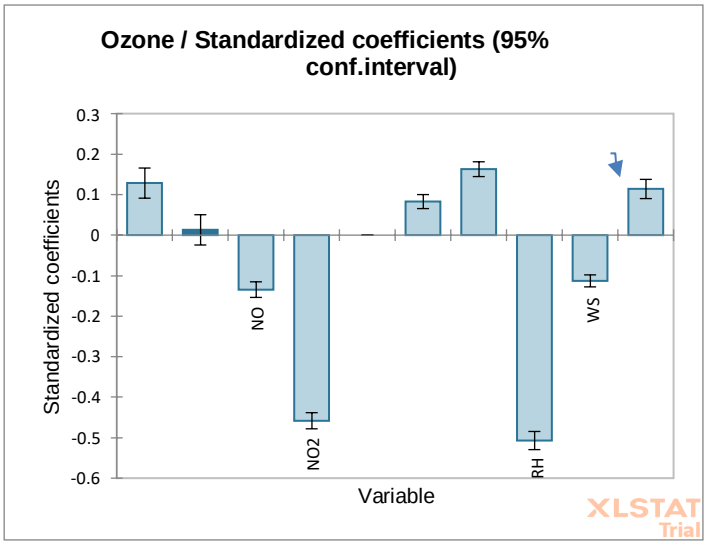

Figure 4.18: β values of each predictor in Nehru Nagar

4. In Dr. Karni Singh Shooting Range the result shows that 56.1% (or adjusted $R^2 = 0.56$) of the variance in O_3 can be accounted for by the other air pollutants and meteorological parameters, collectively, F (9, 9230) = 1313.02, p < 0.0001 as shown in below tables. Looking at the unique individual contributions of the predictors, the results show that $PM_{2.5}$ (β= 0.29, t= 29.9, p < 0.0001), WS (β= 5.7, t= 9.4, p < 0.0001), and temperature (β= 0.14, t= 2.6, p < 0.0001) were among the most significant (p < 0.05) air pollutant and meteorological factors that influenced the incidence of ozone associated with heat wave in Karni which further are portrayed in Equation (4):

Ozone=212.680+0.289*PM$_{2.5}$-0.131*PM$_{10}$-1.863E-02*NO-0.193*NO$_2$-0.582*SO$_2$-11.217*CO-2.114*RH+5.747*WS + 0.141*AT (4)

From the above equation (4) it can be said that with every 1° Celsius rise in atmospheric temperature the surface ozone levels will rise by 0.141. Which further indicates a good positive impact from temperature in the change of ozone levels in Dr. Karni Singh Shooting range.

Table 4.21: Goodness of fit statistics for Dr. Karni Singh Shooting Range

Observations	9240
Sum of weights	9240
DF	9230
R^2	0.561

Adjusted R^2	0.561
MSE	1064.641
RMSE	32.629
MAPE	145.688
DW	0.376
Cp	10.000
AIC	64416.425
SBC	64487.738
PC	0.439
Press	9861585.245
Q^2	0.560

Table 4.22: Analysis of Variance for Dr. Karni Singh Shooting Range

Source	DF	Sum of squares	Mean squares	F	Pr > F
Model	9	12581071.435	1397896.826	1313.022	**<0.0001**
Error	9230	9826635.907	1064.641		
Corrected Total	9239	22407707.342			

Computed against model Y=Mean(Y)

Table 4.23: Model Parameters for Dr. Karni Singh Shooting Range

Source	Value	Standard error	t	Pr > |t|	Lower bound (95%)	Upper bound (95%)
Intercept	212.680	3.521	60.401	**<0.0001**	205.778	219.582
$PM_{2.5}$	0.290	0.010	29.982	**<0.0001**	0.271	0.309
PM_{10}	-0.131	0.007	-20.077	**<0.0001**	-0.144	-0.119
NO	-0.019	0.018	-1.036	0.300	-0.054	0.017
NO_2	-0.193	0.011	-17.802	**<0.0001**	-0.214	-0.172
NOx	0.000	0.000				
SO_2	-0.582	0.053	-10.899	**<0.0001**	-0.687	-0.477
CO	-11.217	0.747	-15.023	**<0.0001**	-12.680	-9.753
RH	-2.114	0.030	-70.241	**<0.0001**	-2.173	-2.055
WS	5.747	0.606	9.482	**<0.0001**	4.559	6.935
AT	0.141	0.052	-2.689	**0.007**	-0.244	-0.038

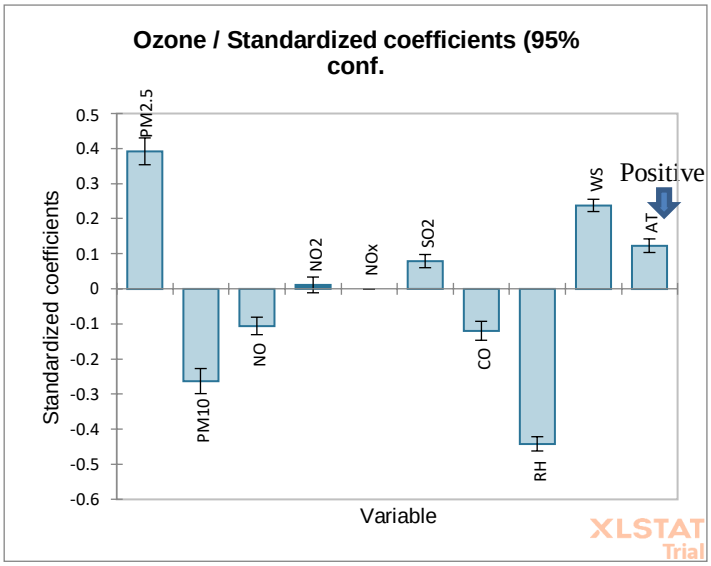

Figure 4.19: β values of each predictor in Dr. Karni Singh Shooting Range

4.6 Discussions

In this study the association between surface-level ozone and all other air pollutants were assessed at all level (univariate, bivariate, and multivariate), the results indicate a moderate inverse correlation of surface ozone with NO, NO_x, NO_2 (ranging around - 0.5), weak to moderate positive correlation with ambient temperature (0.3 to 0.5) and a moderate to strong negative correlation with Relative humidity (-0.6). The correlation results indicate that ambient temperature affects the ozone formation in the atmosphere and act as a precursor. As per Chen et al, 2020, the photochemical oxidation reactions lead to ozone synthesis in troposphere. Formation of ozone follows followingreactions:

$VOC + OH = RO_2 + H_2O$ {in the presence of O_2}

$CO + OH = HO_2 + CO_2$ {in the presence of O_2}

$RO_2 + NO = \text{Secondary VOC} + HO_2 + NO_2$ {in the presence of O_2}

$HO_2 + NO = OH + NO_2$

$NO_2 + \text{sunlight} = NO + O$

$O + O_2 = O_3 + M$

Where, RO_2 – Chain or organic compounds, OH – Hydroxyl Ion, VOC- Volatile Organic Carbon.

The above reactions clearly state the dependence of ozone on NO, NO_2 and NO_x as well as on VOCs. It has been studied that when these nitrogen oxides decrease, the ozone production increases and same is the case for $PM_{2.5}$ (weak inverse correlation).

Also, the ambient temperature is not directly affecting the tropospheric ozone production but it acts as a catalyst for the same. Heat wave associated increase in ozone levels in Delhi may be attributedto the speeding up of photochemical reactions by solar radiations and thus more ozone is observed during afternoon hours of 12:00 to 17:00 hrs. VOCs are root reactants in ozone formation, which react with NO_x on hot sunny days and leads to extraordinary ozone levels. Since, the impact of VOCs on ozone concentrations is more than any other precursor, further study on VOCs and ozone correlation shall be done. Studying role of VOCs on ozone is beyond the scope of this study.

Chapter V

CONCLUSION

In this thesis, the surface ozone concentration of 4 locations in Delhi has been studied. Upon analysis, it was found that the ozone concentration varied from 0.1 to 199.9 μgm^{-3}, 0.72 to 198.8 μgm^{-3}, 0.5 to 199.9 μgm^{-3}, 0.1 to 196.85 μgm^{-3} for Jawahar Lal Nehru Stadium, Dr. Karni Singh Shooting Range, Nehru Nagar and Narela respectively. Ozone concentrations were observed to be highest in afternoon hours (11:00 to 17:00 Hours) when temperature was at peak. The monthly means were maximum for the months of April, May and June with maximum in May 2022 for all the locations. The minimum monthly observations were in January 2022 for Narela and Nehru Nagar, while at JLN stadium and Dr. Karni Singh Shooting Range the minimum values were in August 2021. While the seasonal variations displayed maximum concentrations in summers for all stations which may be attributed to the heat wave situations in Delhi. While the least was observed during monsoon seasons owing to the washout of ozone precursors by precipitation and thereby leading to lesser ozone production. Correlation results showed significant moderate positive association with temperature, and wind speed which indicated that the rise in temperature and wind speed will positively impact the concentration of ozone. Additionally, a weak to moderate significant association with $PM_{2.5}$, PM_{10}, SO_2 and moderate negative significant association with NO, NO_2, NOx, and relative humidity was observed. All 4 monitoring stations have shown significant association between temperature and surface level ozone at multivariate level which further indicates that after excluding the issue of the study indicates a strong dependence of synthesis of surface ozone on nitrogen oxides, VOCs and the solar radiations.

Annexure

NATIONAL AMBIENT AIR QUALITY STANDARDS

S. No.	Pollutant	Time Weighted average	Concentration in Ambient Air		Methods of Measurement
			Industrial, Residential, Rural and Other Area	Ecologically sensitive area (notified by Central Govt.)	
(1)	(2)	(3)	(4)	(5)	(6)
1	Sulphur Dioxide (SO_2), $\mu g/m^3$	Annual*	50	20	• Improved West and Geake • Ultraviolet fluorescence
		24 hours**	80	80	
2	Nitrogen Dioxide (NO_2), $\mu g/m^3$	Annual*	40	30	• Modified Jacob & Hochheiser (Na- Arsenite) • Chemiluminescence
		24 hours**	80	80	
3	Particulate Matter (size less than 10 µm) or $PM_{10} \mu g/m^3$	Annual*	60	60	• Gravimetric • TOEM • Beta attenuation
		24 hours**	100	100	
4	Particulate Matter (size less than 2.5 microns) or $PM_{2.5}$ $\mu g/m^3$	Annual*	40	40	• Gravimetric • TOEM • Beta attenuation
		24 hours**	60	60	
5	Ozone (O_3) $\mu g/m^3$	8 hours **	100	100	• UV photometric • Chemiluminescence • Chemical method
		1 hour **	180	180	
6	Lead (Pb) $\mu g/m^3$	Annual*	0.5	0.5	• ASS / ICP method after sampling on EPM 2000 or equivalent filter paper • ED – XRF using Teflon filter
		24 hours**	1.0	1.0	
(1)	(2)	(3)	(4)	(5)	(6)
7	Carbon Monoxide (CO) mg/m^3	8 hours**	2	2	Non Dispersive Infra RED (NDIR) Spectroscopy
		1 hour**	4	4	
8		Annual*	100	100	

	Ammonia (NH_3) $\mu g/m^3$	24 hours**	400	400	• Chemiluminescence • Indophenol blue method
9	Benzene (C_6H_6) $\mu g/m^3$	Annual*	5	5	• Gas chromatography based continuous analyser • Adsorption and desorption followed by GC analysis
10	Benzo (a) Pyrene (BP) – particulate phase only ng/m^3	Annual*	1	1	Solvent extraction followed by HPLC / GC analysis
11	Arsenic (As) ng/m^3	Annual*	6	6	AAS / ICP method after sampling on EPM 2000 or equivalent filter paper
12	Nickel (Ni) ng/m^3	Annual*	20	20	AAS / ICP method after sampling on EPM 2000 or equivalent filter paper

REFERENCES

Anshika, Kunchala, R. K., Attada, R., Vellore, R. K., Soni, V. K., Mohan, M., & Chilukoti, N. (2021). On the understanding of surface ozone variability, its precursors and their associations with atmospheric conditions over the Delhi region. *Atmospheric Research*, *258*, 105653. https://doi.org/10.1016/j.atmosres.2021.105653

Bloomer, B. J., Stehr, J. W., Piety, C. A., Salawitch, R. J., & Dickerson, R. R. (2009). Observed relationships of ozone air pollution with temperature and emissions. *Geophysical Research Letters*, *36*(9), L09803. https://doi.org/10.1029/2009GL037308

Camalier, L., Cox, W., & Dolwick, P. (2007). The effects of meteorology on ozone in urban areas and their use in assessing ozone trends. *Atmospheric Environment*, *41*(33), 7127–7137. https://doi.org/10.1016/j.atmosenv.2007.04.061

Chen, X., Quéléver, L. L. J., Fung, P. L., Kesti, J., Rissanen, M. P., Bäck, J., Keronen, P., Junninen, H., Petäjä, T., Kerminen, V.-M., & Kulmala, M. (2018). Observations of ozone depletion events in a Finnish boreal forest. *Atmospheric Chemistry and Physics*, *18*(1), 49–63. https://doi.org/10.5194/acp-18-49-2018

Chuwah, C., van Noije, T., van Vuuren, D. P., Stehfest, E., & Hazeleger, W. (2015a). Global impacts of surface ozone changes on crop yields and land use. *Atmospheric Environment*, *106*, 11–23. https://doi.org/10.1016/j.atmosenv.2015.01.062

Chuwah, C., van Noije, T., van Vuuren, D. P., Stehfest, E., & Hazeleger, W. (2015b). Global impacts of surface ozone changes on crop yields and land use. *Atmospheric Environment*, *106*, 11–23. https://doi.org/10.1016/j.atmosenv.2015.01.062

Dufresne, J.-L., Foujols, M.-A., Denvil, S., Caubel, A., Marti, O., Aumont, O., Balkanski, Y., Bekki, S., Bellenger, H., Benshila, R., Bony, S., Bopp, L., Braconnot, P., Brockmann, P.,

Cadule, P., Cheruy, F., Codron, F., Cozic, A., Cugnet, D., … Vuichard, N. (2013). Climate change projections using the IPSL-CM5 Earth System Model: from CMIP3 to CMIP5. *Climate Dynamics*, *40*(9–10), 2123–2165. https://doi.org/10.1007/s00382-012-1636-1

Eyring, V., Arblaster, J. M., Cionni, I., Sedláček, J., Perlwitz, J., Young, P. J., Bekki, S., Bergmann, D., Cameron-Smith, P., Collins, W. J., Faluvegi, G., Gottschaldt, K.-D., Horowitz, L. W., Kinnison, D. E., Lamarque, J.-F., Marsh, D. R., Saint-Martin, D., Shindell, D. T., Sudo, K., … Watanabe, S. (2013). Long-term ozone changes and associated climate impacts in CMIP5 simulations. *Journal of Geophysical Research: Atmospheres*, *118*(10), 5029–5060. https://doi.org/10.1002/jgrd.50316

Fiore, A. M., Naik, V., & Leibensperger, E. M. (2015). Air Quality and Climate Connections. *Journal of the Air & Waste Management Association*, *65*(6), 645–685. https://doi.org/10.1080/10962247.2015.1040526

Fleming, Z. L., Doherty, R. M., von Schneidemesser, E., Malley, C. S., Cooper, O. R., Pinto, J. P., Colette, A., Xu, X., Simpson, D., Schultz, M. G., Lefohn, A. S., Hamad, S., Moolla, R., Solberg, S., & Feng, Z. (2018). Tropospheric Ozone Assessment Report: Present-day ozone distribution and trends relevant to human health. *Elementa: Science of the Anthropocene*, *6*. https://doi.org/10.1525/elementa.273

Ghude, S. D., Jain, S. L., Arya, B. C., Beig, G., Ahammed, Y. N., Kumar, A., & Tyagi, B. (2008). Ozone in ambient air at a tropical megacity, Delhi: characteristics, trends and cumulative ozone exposure indices. *Journal of Atmospheric Chemistry*, *60*(3), 237–252. https://doi.org/10.1007/s10874-009-9119-4

Hakkim, H., Sinha, V., Chandra, B. P., Kumar, A., Mishra, A. K., Sinha, B., Sharma, G., Pawar, H., Sohpaul, B., Ghude, S. D., Pithani, P., Kulkarni, R., Jenamani, R. K., & Rajeevan, M. (2019). Volatile organic compound measurements point to fog-induced biomass burning

feedback to air quality in the megacity of Delhi. *Science of The Total Environment*, *689*, 295–304. https://doi.org/10.1016/j.scitotenv.2019.06.438

Hendriks, C., Forsell, N., Kiesewetter, G., Schaap, M., & Schöpp, W. (2016). Ozone concentrations and damage for realistic future European climate and air quality scenarios. *Atmospheric Environment*, *144*, 208–219. https://doi.org/10.1016/j.atmosenv.2016.08.026

Huang, G., Liu, X., Chance, K., Yang, K., Bhartia, P. K., Cai, Z., Allaart, M., Ancellet, G., Calpini, B., Coetzee, G. J. R., Cuevas-Agulló, E., Cupeiro, M., de Backer, H., Dubey, M. K., Fuelberg, H. E., Fujiwara, M., Godin-Beekmann, S., Hall, T. J., Johnson, B., … Yela, M. (2017). Validation of 10-year SAO OMI Ozone Profile (PROFOZ) product using ozonesonde observations. *Atmospheric Measurement Techniques*, *10*(7), 2455–2475. https://doi.org/10.5194/amt-10-2455-2017

Lamarque, J.-F. (2005). Tropospheric ozone evolution between 1890 and 1990. *Journal of Geophysical Research*, *110*(D8), D08304. https://doi.org/10.1029/2004JD005537

Levy, B. S., & Patz, J. A. (2015). Climate Change, Human Rights, and Social Justice. *Annals of Global Health*, *81*(3), 310. https://doi.org/10.1016/j.aogh.2015.08.008

Li, K., Jacob, D. J., Liao, H., Shen, L., Zhang, Q., & Bates, K. H. (2019). Anthropogenic drivers of 2013–2017 trends in summer surface ozone in China. *Proceedings of the National Academy of Sciences*, *116*(2), 422–427. https://doi.org/10.1073/pnas.1812168116

Liao, Z., Ling, Z., Gao, M., Sun, J., Zhao, W., Ma, P., Quan, J., & Fan, S. (2021). Tropospheric Ozone Variability Over Hong Kong Based on Recent 20 years (2000–2019) Ozonesonde Observation. *Journal of Geophysical Research: Atmospheres*, *126*(3). https://doi.org/10.1029/2020JD033054

Liu, J., Rodriguez, J. M., Steenrod, S. D., Douglass, A. R., Logan, J. A., Olsen, M. A., Wargan, K., & Ziemke, J. R. (2017). Causes of interannual variability over the southern hemispheric tropospheric ozone maximum. *Atmospheric Chemistry and Physics*, *17*(5), 3279–3299. https://doi.org/10.5194/acp-17-3279-2017

Lombardozzi, D., Levis, S., Bonan, G., Hess, P. G., & Sparks, J. P. (2015). The Influence of Chronic Ozone Exposure on Global Carbon and Water Cycles. *Journal of Climate*, *28*(1), 292–305. https://doi.org/10.1175/JCLI-D-14-00223.1

Lu, X., Zhang, L., Chen, Y., Zhou, M., Zheng, B., Li, K., Liu, Y., Lin, J., Fu, T.-M., & Zhang, Q. (2019). Exploring 2016–2017 surface ozone pollution over China: source contributions and meteorological influences. *Atmospheric Chemistry and Physics*, *19*(12), 8339–8361. https://doi.org/10.5194/acp-19-8339-2019

Lu, X., Zhang, L., Wang, X., Gao, M., Li, K., Zhang, Y., Yue, X., & Zhang, Y. (2020a). Rapid Increases in Warm-Season Surface Ozone and Resulting Health Impact in China Since 2013. *Environmental Science & Technology Letters*, *7*(4), 240–247. https://doi.org/10.1021/acs.estlett.0c00171

Lu, X., Zhang, L., Wang, X., Gao, M., Li, K., Zhang, Y., Yue, X., & Zhang, Y. (2020b). Rapid Increases in Warm-Season Surface Ozone and Resulting Health Impact in China Since 2013. *Environmental Science & Technology Letters*, *7*(4), 240–247. https://doi.org/10.1021/acs.estlett.0c00171

Meehl, G. A., & Tebaldi, C. (2004). More Intense, More Frequent, and Longer Lasting Heat Waves in the 21st Century. *Science*, *305*(5686), 994–997. https://doi.org/10.1126/science.1098704

PAI, D. S., NAIR, S., & RAMANATHAN, A. N. (2013). Long term climatology and trends of heat waves over India during the recent 50 years (1961-2010). *MAUSAM*, *64*(4), 585–604. https://doi.org/10.54302/mausam.v64i4.742

Perkins-Kirkpatrick, S. E., & Gibson, P. B. (2017). Changes in regional heatwave characteristics as a function of increasing global temperature. *Scientific Reports*, *7*(1), 12256. https://doi.org/10.1038/s41598-017-12520-2

Pfister, G. G., Walters, S., Lamarque, J.-F., Fast, J., Barth, M. C., Wong, J., Done, J., Holland, G., & Bruyère, C. L. (2014). Projections of future summertime ozone over the U.S. *Journal of Geophysical Research: Atmospheres*, *119*(9), 5559–5582. https://doi.org/10.1002/2013JD020932

Phalitnonkiat, P., Hess, P. G. M., Grigoriu, M. D., Samorodnitsky, G., Sun, W., Beaudry, E., Tilmes, S., Deushi, M., Josse, B., Plummer, D., & Sudo, K. (2018). Extremal dependence between temperature and ozone over the continental US. *Atmospheric Chemistry and Physics*, *18*(16), 11927–11948. https://doi.org/10.5194/acp-18-11927-2018

Qu, Y., Voulgarakis, A., Wang, T., Kasoar, M., Wells, C., Yuan, C., Varma, S., & Mansfield, L. (2021). A study of the effect of aerosols on surface ozone through meteorology feedbacks over China. *Atmospheric Chemistry and Physics*, *21*(7), 5705–5718. https://doi.org/10.5194/acp-21-5705-2021

Sharma, S., Barrie, L. A., Magnusson, E., Brattström, G., Leaitch, W. R., Steffen, A., & Landsberger, S. (2019). A Factor and Trends Analysis of Multidecadal Lower Tropospheric Observations of Arctic Aerosol Composition, Black Carbon, Ozone, and Mercury at Alert, Canada. *Journal of Geophysical Research: Atmospheres*, *124*(24), 14133–14161. https://doi.org/10.1029/2019JD030844

Shen, L., Mickley, L. J., & Gilleland, E. (2016). Impact of increasing heat waves on U.S. ozone episodes in the 2050s: Results from a multimodel analysis using extreme value theory. *Geophysical Research Letters*, *43*(8), 4017–4025. https://doi.org/10.1002/2016GL068432

Silver, B., Reddington, C. L., Arnold, S. R., & Spracklen, D. v. (2018). Substantial changes in air pollution across China during 2015–2017. *Environmental Research Letters*, *13*(11), 114012. https://doi.org/10.1088/1748-9326/aae718

Steiner, A. L., Davis, A. J., Sillman, S., Owen, R. C., Michalak, A. M., & Fiore, A. M. (2010). Observed suppression of ozone formation at extremely high temperatures due to chemical and biophysical feedbacks. *Proceedings of the National Academy of Sciences*, *107*(46), 19685–19690. https://doi.org/10.1073/pnas.1008336107

Sun, W., Hess, P., & Liu, C. (2017). The impact of meteorological persistence on the distribution and extremes of ozone. *Geophysical Research Letters*, *44*(3), 1545–1553. https://doi.org/10.1002/2016GL071731

van Vuuren, D. P., Edmonds, J., Kainuma, M., Riahi, K., Thomson, A., Hibbard, K., Hurtt, G. C., Kram, T., Krey, V., Lamarque, J.-F., Masui, T., Meinshausen, M., Nakicenovic, N., Smith, S. J., & Rose, S. K. (2011). The representative concentration pathways: an overview. *Climatic Change*, *109*(1–2), 5–31. https://doi.org/10.1007/s10584-011-0148-z

Wang, T., Xue, L., Brimblecombe, P., Lam, Y. F., Li, L., & Zhang, L. (2017). Ozone pollution in China: A review of concentrations, meteorological influences, chemical precursors, and effects. *Science of The Total Environment*, *575*, 1582–1596. https://doi.org/10.1016/j.scitotenv.2016.10.081